Published in : Biochemical Pharmacology (2024), vol. 220, 116013
DOI: 10.1016/j.bcp.2023.116013
Status : Postprint (Author's version)

BASAL INTERACTION OF THE ORPHAN RECEPTOR GPR101 WITH ARRESTINS LEADS TO CONSTITUTIVE INTERNALIZATION

Grégory Dayana Abboud [a], Clauda Abboud [a], Asuka Inoue [b], Jean-Claude Twizere [c], Julien Hanson [a d1]

[a] *Laboratory of Molecular Pharmacology, GIGA-Molecular Biology of Diseases, University of Liege, Liege, Belgium*
[b] *Graduate School of Pharmaceutical Sciences, Tohoku University, Sendai, Miyagi, Japan*
[c] *Laboratory of Viral Interactomes, GIGA-Molecular Biology of Diseases, University of Liege, Liege, Belgium*
[d] *Laboratory of Medicinal Chemistry, Center for Interdisciplinary Research on Medicines (CIRM), University of Liege, Liege, Belgium*

KEYWORDS : Orphan GPCR ; GPR101 ; Arrestin ; Internalization ; Constitutive activity ; Clathrin

ABSTRACT

GPR101 is an orphan G protein-coupled receptor that promotes growth hormone secretion in the pituitary. The microduplication of the GPR101 gene has been linked with the X-linked acrogigantism, or X-LAG, syndrome. This disease is characterized by excessive growth hormone secretion and abnormal rapid growth beginning early in life. Mechanistically, GPR101 induces growth hormone secretion through constitutive activation of multiple heterotrimeric G proteins. However, the full scope of GPR101 signaling remains largely elusive. Herein, we investigated the association of GPR101 to multiple transducers and uncovered an important basal interaction with Arrestin 2 (β-arrestin 1) and Arrestin 3 (β-arrestin 2). By using a GPR101 mutant lacking the C-terminus and cell lines with an Arrestin 2/3 null background, we show that the arrestin association leads to constitutive clathrin- and dynamin-mediated GPR101 internalization. To further highlight GPR101 intracellular fate, we assessed the colocalization of GPR101 with Rab protein markers. Internalized GPR101 was mainly colocalized with the early endosome markers, Rab5 and EEA-1, and to a lesser degree with the late endosome marker Rab7. However, GPR101 was not colocalized with the recycling endosome marker Rab11. These findings show that the basal arrestin recruitment by GPR101 C-terminal tail drives the receptor constitutive clathrin-mediated internalization.

Abbreviations: AC, Adenylate cyclase; AF488, Alexa Fluor 488; AKAP, A-kinase anchor protein; Ala, Alanine; AP-2, β2 adaptin subunit of adaptor protein-2; AVP, Vasopressin; β2AR, β2-adrenoceptor; cAMP, Cyclic adenosine monophosphate; CCF, Cross-correlation factor; CHX, Cycloheximide; Co-IP, Co-immunoprecipitation; CRISPR/Cas 9, Clustered regularly interspaced short palindromic repeats/CRISPR-associated protein 9; DAG, Diacylglycerol; EEA-1, Early endosome antigen-1; ER, Endoplasmic reticulum; FEME, Fast endophilin-mediated endocytosis; FLuc, Firefly luciferase; GEF, Guanine nucleotide exchange; GFP, Green fluorescent protein; GH, Growth hormone; GPCR, G protein-coupled receptor; GRKs, GPCR kinases; HA, Hemagglutinin; HEK293, Human embryonic kidney 293; ICL, Intracellular loop; IP3, Inositol triphosphate; ISO, Isoproterenol; LgBiT, Large subunit of the nanoluciferase enzyme; NLuc, Nanoluciferase; PKA, Protein kinase A; PKC, Protein kinase C; Ser, Serine; Thr, Threonine; V1aR, Vasopressin 1a receptor; V1P1R, Vasoactive intestinal peptide 1 receptor; V2R, Vasopressin 2 receptor; WB, Western blot; WGA, Wheat germ agglutinin; WT, Wild-type; X-LAG, X-linked acrogigantism.

Published in : Biochemical Pharmacology (2024), vol. 220, 116013
DOI: 10.1016/j.bcp.2023.116013
Status : Postprint (Author's version)

Intracellularly, GPR101 concentrates in the endosomal compartment and is degraded through the lysosomal pathway. In conclusion, we uncovered a constitutive intracellular trafficking of GPR101 that potentially represents an important layer of regulation of its signaling and function.

1. Introduction

GPR101 is a G protein-coupled receptor (GPCR) that has no known validated endogenous ligand and is thus considered orphan[1], [2]. GPCRs constitute the largest family of membrane proteins (350 members, excluding the 500 olfactory receptors) and are implicated in virtually all physiological processes. GPCRs attract a lot of interest due to their impressive track record as drug targets. Indeed, as much as 30 % of our therapeutic arsenal targets one of them directly[3]. However, many members of the family are understudied and have an elusive function and more than 100 of them are still orphan[4]. Thus, the elucidation of GPCR signaling and function as well as the discovery of their ligand is highly relevant in health and diseases.

On the cell surface, GPCRs act as information hubs across the membrane. Their activation by extracellular ligands trigger signaling pathway and a cellular response to changing environment. Most of them share a common activation scheme where different conformations spontaneously adopted by the receptors are stabilized and enriched by ligands. Active conformations bind to heterotrimeric G proteins composed of a G_{α} and a $G_{\beta\gamma}$ subunits that exchange their G_{α} bound GDP for a GTP and dissociate to propagate the signal[5]. Various pathways can be activated depending on the nature of the G_{α} subunits: $G_{i/o}$ and G_s modulate negatively and positively adenylate cyclase (AC) and cyclic adenosine monophosphate (cAMP) levels, $G_{q/11}$ leads to the release of diacylglycerol (DAG) and inositol triphosphate (IP_3) that results in $[Ca^{2+}]_i$ release from internal stores while $G_{12/13}$ notably drives RhoA activation through the binding and stimulation of Rho-guanine nucleotide exchange (GEF) factors[6].

Active ligand-receptor complexes can be phosphorylated, on the intracellular loop (ICL) 3 and the C-terminal tail, principally by GPCR kinases (GRKs), protein kinase A (PKA) and protein kinase C (PKC), triggering arrestin recruitment[7]. These scaffolding proteins desensitize the receptor by blocking G protein coupling and promote the internalization of the receptor[8]. Four arrestins have been described, Arrestin 1 and 4 that are only found in retinal tissues and Arrestin 2 and 3 (also known as β-Arrestin 1 and 2, respectively) that have an ubiquitous expression[9]. Besides their role in desensitization and internalization, arrestins also contribute to downstream GPCR signaling, although G proteins are required to initiate arrestin-mediated signaling[10], [11], [12], [13]. The most well characterized mechanism for arrestin-triggered internalization involves the recruitment to clathrin-coated pits through interactions with the β2 adaptin subunit of adaptor protein-2 (AP-2)[14]. A simplified classification proposes that two main types of GPCRs exist regarding their interactions with arrestins. Class A [β_2 adrenergic receptor (β_2AR), vasopressin 1a receptor (V1aR), …] transiently interact with arrestins and are rapidly recycled back to the membrane while class B [Vasopressin V2 receptor (V_2R), Prostaglandin EP4 receptor, vasoactive intestinal peptide 1 receptor (V1P1R), …] form more stable complexes and display a slow recycling profile or are degraded[15],

Published in : Biochemical Pharmacology (2024), vol. 220, 116013
DOI: 10.1016/j.bcp.2023.116013
Status : Postprint (Author's version)

[16]. In addition to their different intracellular fate, class A have greater affinity for Arrestin 3 over Arrestin 2 while class B display a more balanced affinity profile between the two non-visual arrestins[15]. Beside these well-established processes, various reports have demonstrated that GPCRs can also be internalized through clathrin-coated pits in an arrestin-independent manner[17], [18], [19]. In addition, the use of non-coated vesicles in an arrestin-dependent or independent manner has been described[20]. These alternative clathrin-independent internalization mechanisms rely for example on the formation of caveolae[21], [22], [23], [24] or the newly described fast endophilin-mediated endocytosis (FEME) pathway[25]. Once internalized, the receptor is typically sorted to different endocytic compartments, that can be delineated with the small GTPases Rab[26]. Rab5 plays important roles in directing GPCRs from the plasma membrane to the intracellular compartment and are typically used as markers for early endosomes. Rab7 participates to the formation of late endosomes (or lysosomes) that are part of the receptor degradation pathway, while Rab11 and Rab4 are markers for the slow and fast recycling pathway, respectively[27].

GPR101 is predominantly expressed in the brain, notably in the hypothalamus, but also in other tissues such as the pituitary[28], [29]. In 2014, a microduplication of the locus (Xq26.3) containing the GPR101 gene was shown to be associated with the X-linked acrogigantism (X-LAG) syndrome[30], [31]. This aggressive disease is characterized by infant-onset growth hormone (GH) hypersecretion, pituitary hyperplasia and tumorigenesis[32]. Recently, we provided seminal insights into the GPR101 signaling by showing that it is coupled to three families of G proteins, namely G_s, $G_{q/11}$ and $G_{12/13}$. Furthermore, we showed that in somatotropes, the specialized pituitary GH-secreting cells, GPR101 drives GH secretion through the constitutive activation of both G_s and $G_{q/11}$ and plays a relevant role in the control of growth in health and disease[29]. Interestingly, these pro-secreting effects are observed with no GPR101-mediated effects on cell proliferation, although it is a traditional hallmark of G_s overactivation in somatotropes, suggesting a compartmentalized signaling. Notwithstanding, the functions of GPR101 seem to be linked to its high level of constitutive activity, which is the capacity for a GPCR to signal in the absence of ligands[28], [29].

Given its high potential as an innovative drug target and its established role in GH secretion, we sought to gain additional insight into GPR101 primary coupling and how it impacts its cellular location and trafficking.

In the present study, we identified through different pharmacological assays that GPR101 recruits both Arrestin 2 and 3 in a constitutive manner. We performed antibody feeding experiments and imaging to show that GPR101 is constitutively internalized. Furthermore, by using Arrestin 2/3-depleted cells and GPR101 mutants devoid of arrestin recruitment capabilities, we evidenced that this internalization is the result of the basal arrestin binding to the receptor. Post-endocytic sorting analysis revealed that GPR101 is mainly directed through the clathrin pathway to degradation.

Published in : Biochemical Pharmacology (2024), vol. 220, 116013
DOI: 10.1016/j.bcp.2023.116013
Status : Postprint (Author's version)

2. Materials and methods

2.1. REAGENTS

All chemicals were purchased from Sigma-Aldrich (St. Louis, MO, USA) unless otherwise stated. The following commercially available antibodies were used for several applications: anti-FLAG clone M2 (mouse, Cat. No F3165) from Sigma-Aldrich (St. Louis, MO, USA), anti-HA tag (rabbit, Cat. No 3724), Anti-HSP90 (rabbit, Cat. No 4877), anti-VCL (rabbit, Cat. No 13901), anti-mouse IgG (H + L) F(ab')2 Fragment AF488 Conjugate (Cat. No 4408), rabbit anti-GM130 antibody (Cat. No 12480 T), anti-rabbit IgG Fab2 AF647 (Cat No 4414), anti-mouse IgG horseradish peroxidase (HRP)-linked antibody (Cat. No 7076) and anti-rabbit IgG HRP-linked antibody (Cat. No 7074) from Cell Signaling Technology (Danvers, MA, USA). The endosomal marker antibody sampler kit (Cat. No 12666) containing monoclonal antibodies against the human caveolin-1, human clathrin heavy chain protein, human EEA-1 protein, human Rab5A protein, human Rab7 protein and human Rab11 protein, was purchased from Cell Signaling Technology (Danvers, MA, USA). D-luciferin sodium salt (Cat. No 14682) was from Cayman Chemicals (Ann Arbor, MI, USA). Coelenterazine-h (Cat. No 1-361304-200) was from Regis Technologies (Morton Grove, IL, USA).

2.2. MOLECULAR CLONING AND PLASMID CONSTRUCTION

Human GPR101 and β_2AR were amplified from human embryonic kidney 293 (HEK293) cell genomic DNA. Vasopressin 2 receptor (V_2R) was amplified from Human ORFeome (Version 7.1, https://horfdb.dfci.harvard.edu/hv7/). All receptors were cloned into the pIRESpuro vector (Clontech Laboratories, Mountain View, CA, USA) (for stable transfections) and/or pcDNA3.1 (Invitrogen Corporation, Carlsbad, CA, USA) (for transient transfections) after addition of the FLAG epitope (DYKDDDDK) at the N-terminus, unless specified otherwise.

GPR101 and V_2R were cloned directly into the firefly luciferase assay vector containing a linker (L) and firefly luciferase amino acid 413–549 (Fc) (already described in[33], [34]) to give GPR101-LFc and V_2R-LFc constructs. Human Arrestin 2 was amplified from HEK293 cDNA, rat Arrestin 3 from Arrestin 3-GFP and fused with a linker (L) and firefly luciferase amino acid 1–415 (Fn) to give arrestin 2/3-FnL constructs[33], [34]. The pGloSensorTM-22F cAMP (cAMP GloSensorTM) plasmid was obtained from Promega Corporation (Madison, WI, USA). The following plasmids were from Addgene (Cambridge, MA, USA): HA-Dynamin 1 K44A (#34683, a gift from Sandra Schmid), Arrestin 3-GFP (#35411, a gift from Robert Lefkowitz[35]) Sec16B-GFP (#66607, a gift from David Stephens[36]) and Sec23A-GFP (#66609, a gift from David Stephens[37]). AKAP-RFP was a generous gift from Dr. Stephanie Herkenne. G_s-LgBiT, G_q-LgBiT, G_{11}-LgBiT, G_{12}-LgBiT, G_{13}-LgBiT, G_z-LgBiT, G_o-LgBiT, G_{i1}-LgBiT, G_{i2}-LgBiT, G_{i3}-LgBiT and Arrestin 3-LgBiT constructs are already described [38], [39]. For GPR101-NP, a small fragment of the nanoluciferase enzyme (NP) was fused at the C-terminus of the GPR101 sequence, preceded by a flexible linker (sequence: GGGAATTCTGGCTCGAGCGGTGGTGGCGGGAGCGGAGGTGGAGGGTCGTCAGGT), yielding GPR101-NP construct. A FLAG epitope was added to the N-terminus of the GPR101 sequence. Mutations and

Published in : Biochemical Pharmacology (2024), vol. 220, 116013
DOI: 10.1016/j.bcp.2023.116013
Status : Postprint (Author's version)

truncations were introduced by using the Q5 Site-Directed Mutagenesis Kit (Cat. No E0554S, New England Biolabs, MA, USA). The sequence of all plasmids was validated by sanger sequencing (GIGA genomic platform, Liege, Belgium).

2.3. CELL CULTURE AND TRANSFECTION

HEK293 cells (ATCC, Manassas, VA, USA) were grown in Dulbecco's Modified Eagle Medium (DMEM, Cat. No L0106, Biowest, Nuaillé, France) supplemented with 10 % fetal bovine serum (FBS, Cat. No P40-37500, lot P160105, International Medical Products, Belgium), 1 % penicillin/streptomycin (Cat. No DE17-603E, Lonza, Basel, Switzerland) and 2 mM L-glutamine (Cat. No 0550, Biowest, Nuaillé, France) at 37 °C and 5 % CO_2. Stable FnL-arrestin 3 and pGlo HEK293 cell lines were selected with hygromycin B Gold (320 µg ml^{-1}, InvivoGen, San Diego, CA, USA) and puromycin (1 µg ml^{-1}, InvivoGen, San Diego, CA, USA). The resulting clones were selected for expression of GPR101 and arrestin by FACS analysis. CRISPR/Cas 9 generated HEK293 ΔArrestin 2/3 have been described previously[39], [40]. For transient transfections, 48 h before the experiment, cells were transfected with plasmids using calcium phosphate precipitation method, unless stated otherwise. All experiment were carried out with cells between passage 3 and 15. In the current study, we rely on a single cell type as we do not investigate the biology of HEK293 cells but use them as recipient for transfected receptors.

2.4. GLOSENSOR CAMP ASSAY

Variations of cAMP levels were measured with the GloSensor™ technique according to the manufacturer's instructions (Promega Corporation, Madison, WI, USA) and previous description[40], [41]. Briefly, HEK293 cells stably expressing the GloSensor plasmid 22F were transiently transfected with 15 µg of plasmid containing GPR101 (WT or △Cter mutant). 48 h later, cells were detached and incubated 1 h in the dark at 37 °C in HBSS assay buffer (120 mM NaCl, 5.4 mM KCl, 0.8 mM $MgSO_4$, 10 mM HEPES; pH 7.4, 10 mM glucose) containing 3-isobutyl-1-methylxanthin (IBMX, 100 µM) and D-luciferin (50 µM). Then, 100,000 cells per well were distributed into 96-well plates (Cat. No 655075, microplate, PS, 96-well, F-bottom, white, lumitrac, Greiner bio-one, Kremsmünster, Austria). Luminescence was directly recorded for 30 min on a Centro XS3 LB 960 reader (Berthold Technologies, Bad Wildbad, Germany). For endocytosis experiments, FLAG-GPR101-transfected cells were treated with various concentrations of dynasore (0.1, 1, 10 and 50 µM) or vehicle (1 %DMSO) for 30 min at 37 °C, before measuring luminescence.

2.5. MEASUREMENT OF G PROTEIN OR ARRESTIN 3 RECRUITMENT AT THE GPR101 RECEPTOR WITH THE NANOLUCIFERASE COMPLEMENTATION ASSAY

HEK293 cells were seeded in 10 cm dishes and they were co-transfected with 7.5 µg GPR101-NP or empty plasmid (MOCK condition) and either the G protein (G_s, G_q, G_{11}, G_{12}, G_{13}, G_z, G_o, G_{i1}, G_{i2} or G_{i3})-LgBiT or the Arrestin 3-LgBiT plasmids. 24 h later, cells were detached and medium was replaced by phosphate-buffered saline (PBS) solution containing the nanoluciferase substrate (Coelenterazine-

Published in : Biochemical Pharmacology (2024), vol. 220, 116013
DOI: 10.1016/j.bcp.2023.116013
Status : Postprint (Author's version)

h, 5 µM). After a 30 min incubation at 37 °C, cells were distributed in 96-well plates (Cat. No 655075, microplate, PS, 96-well, F-bottom, white, lumitrac, Greiner bio-one, Kremsmünster, Austria) at a density of 50,000 cells per well, and luminescence was directly recorded for 30 min on a Centro XS3 LB 960 reader (Berthold Technologies, Bad Wildbad, Germany).

2.6. MEASUREMENT OF ARRESTIN RECRUITMENT BY THE FIREFLY LUCIFERASE COMPLEMENTATION ASSAY

HEK293 cells stably expressing FnL-Arrestin 3 or transiently transfected with FnL-Arrestin 2 were transfected with different amounts (0, 7.5, 15 and 30 µg) of the plasmid DNA coding for GPR101 (WT or mutants) or other receptors (V_2R WT, V_2R R3.50H) fused to the C-terminal part of the luciferase (GPCR-LFc) in 10 cm dishes. After 48 h incubation, cells were detached and medium was replaced with HBSS buffer (120 mM NaCl, 5.4 mM KCl, 0.8 mM $MgSO_4$, 10 mM HEPES; pH 7.4). After addition of D-luciferin (50 µM), luminescence was measured for 30 min on a Centro XS3 LB960 plate reader (Berthold Technologies, Bad Wildbad, Germany).

2.7. DETERMINATION OF RECEPTOR EXPRESSION BY FLOW CYTOMETRY

The expression level of FLAG-GPR101 (WT or mutants) or other receptors was determined using flow cytometry. In brief, cells were seeded in 10 cm dishes and 24 h later transfected with various amounts of receptor plasmids (0, 7.5, 15 and 30 µg). 48 h after, cells were detached, washed, and incubated with a primary mouse monoclonal anti-FLAG antibody (1:1000) for 45 min at 4 °C in FACS buffer [1 % bovine serum albumin (BSA) in PBS]. After washing, cells were incubated with AF488-conjugated anti-mouse antibody (1:1000) in FACS buffer for 45 min at 4 °C in the dark. For the determination of total expression, cells were fixed for 40 min in 1 % paraformaldehyde (PFA) at 4 °C, and then incubated for 15 min with 0.3 % saponin (Cat. No S4521, Sigma-Aldrich, St. Louis, MO, USA) at 4 °C in FACS buffer to allow cell permeabilization, before antibody addition [mouse anti-FLAG (1:1000) and AF488-coupled anti-mouse antibody (1:1000)]. After several washing steps, cells were left in 200 µl FACS buffer, and analyzed using the FACSVerse™ flow cytometer (BD Biosciences, Franklin Lakes, NJ, USA). Data were acquired on the FlowJo™ software (BD Biosciences, Franklin Lakes, NJ, USA).

2.8. IMMUNOFLUORESCENCE

FLAG-GPR101-expressing HEK293 cells were grown on poly-D-lysine treated glass coverslips at 37 °C in 5 % CO2 for 24 h. After washing with PBS, cells were fixed for 10 min at room temperature in PBS containing 4 % PFA. Then, cells were incubated with 50 mM NH_4Cl to quench the fluorescence. Cells were permeabilized at room temperature for 15 min with PBS containing 0.5 % saponin. After wash, cells were blocked in PBS containing 5 % FBS and 0.5 % saponin for 60 min, and then incubated with an anti-FLAG antibody (1:1000) and each of the endosomal markers [clathrin (1:50), caveolin-1 (1:200), Rab5A (1:200), EEA-1 (1:200), Rab7 (1:100) and Rab11 (1:50)] diluted in blocking buffer for 2 h at room temperature. Cells were subsequently washed three times in PBS prior to incubation with

Published in : Biochemical Pharmacology (2024), vol. 220, 116013
DOI: 10.1016/j.bcp.2023.116013
Status : Postprint (Author's version)

secondary antibodies. Anti-mouse AF488-conjugated antibody (1:1000 dilution) was used for detection of FLAG-tagged receptors while anti-rabbit AF647-conjugated antibody (1:1000 dilution) was used for detection of endosomal markers. After 2 h of incubation at room temperature, cells were washed three times in PBS and glass coverslips were mounted using ProLong™ Gold Antifade Mountant containing DAPI (Cat. No P36931, ThermoFisher Scientific, Waltham, MA, USA).

For the plasma membrane staining, cells were washed, fixed and subsequently incubated with wheat germ agglutinin (WGA, AF647 conjugate, 5 µg ml^{-1}, Cat. No W32466, ThermoFisher Scientific, Waltham, MA, USA) at 37 °C for 10 min, before antibody staining.

For colocalization with Arrestin 3, FLAG-GPR101-expressing HEK293 cells were transfected with Arrestin 3-GFP plasmid and receptor labeling was performed by using a primary rabbit anti-FLAG antibody (1:1000 dilution) and a secondary anti-rabbit antibody conjugated to AF647 (1:1000 dilution).

For endocytosis inhibition studies, FLAG-GPR101-expressing HEK293 were transfected with pcDNA3.1 HA-Dynamin 1 K44A or treated with pitstop 2 (25 µM, Cat. No SML1169, Sigma-Aldrich, St. Louis, MO, USA), dynasore (50 µM, Cat. No 324410, Sigma-Aldrich, St. Louis, MO, USA), chloroquine (200 µM, Cat. No C6628, Sigma-Aldrich, St. Louis, MO, USA) and hyperosmotic sucrose (0.5 M, Cat. No S0389, Sigma-Aldrich, St. Louis, MO, USA) for 30 min at 37 °C in the assay buffer (20 mM HEPES at pH 7.5, 140 mM NaCl, 1 mM CaCl2, 1 mM MgSO4, 5.5 mM glucose and 0.5 % BSA) before the immunofluorescence staining. The cycloheximide (CHX, Cat. No C7698, Sigma-Aldrich, St. Louis, MO, USA) was used at a concentration of 10 µg ml^{-1} for 4 h in a serum-free medium, while MG132 (Cat. No C2211, Sigma-Aldrich) and Heclin (Cat. No SML1396, Sigma-Aldrich) were used at a concentration of 10 µM for 2 h at 37 °C. Cells were visualized and image acquisition was performed on a NIKON A1R (Nikon, Shinjuku, Tokyo, Japan) confocal microscope (oil immersion objective, ×60 magnification).

2.9. ANTIBODY FEEDING INTERNALIZATION

For receptor internalization assays, HEK293 cells stably expressing FLAG-GPR101 were cultured in 10 cm plates and serum-starved before experiment. Cell surface receptors were labeled with a mouse anti-FLAG antibody (1:1000 dilution) for 30 min on ice in assay buffer (DMEM, 0.5 % BSA, 10 mM HEPES, pH 7.4). The unbound antibody was washed away with cold assay buffer, and then cells were incubated in assay buffer at 37 °C for different periods of time (0, 5, 15, 30, 45, 60 and 75 min). Cells were washed with PBS containing 0.5 % BSA, and the remaining cell surface receptors were detected with an anti-mouse antibody conjugated to AF488 (1:1000 dilution). The relative amount of receptor remaining on the surface at each time point was quantified using the FACSVerse™ flow cytometer (BD Biosciences, Franklin Lakes, NJ, USA) and analyzed using FlowJo software (BD Biosciences, Franklin Lakes, NJ, USA). FLAG-β_2AR expressing HEK293 cells were serum-starved for 30 min and then treated with vehicle or Isoproterenol (ISO, 10 µM) for 15 min at 37 °C. Following internalization of the receptor, cells were washed three times (to remove cell surface-bound ligand) and incubated in assay buffer at 37 °C for 35 min to detect recycling levels of the receptor.

Published in : Biochemical Pharmacology (2024), vol. 220, 116013
DOI: 10.1016/j.bcp.2023.116013
Status : Postprint (Author's version)

2.10. CO-IMMUNOPRECIPITATION

HEK293 cells were seeded in 10 cm culture dishes and co-transfected with 15 µg of FLAG-GPR101 (or empty vector MOCK) and 15 µg of HA-tagged Arrestin 2 (or Arrestin 3) constructs in pcDNA3.1 vectors. 48 h after transfection, cells were serum-starved and washed with ice-cold PBS and homogenized in cold RIPA lysis buffer (Cat. No 89900, ThermoFisher Scientific, Waltham, MA, USA) containing 1 % of protease (Cat. No 04694159001, Roche, Basel, Switzerland) and phosphatase (Cat. No 04906837001, Roche, Basel, Switzerland) inhibitors for 30 min at 4 °C. The homogenates were placed on a rotator for 30 min at 4 °C and clarified by centrifugation 10 min at 10,000 × g and 4 °C. An aliquot of the supernatant fraction was used for analysis of the total cell lysate (input) and the remaining sample (900µg) was used for co-immunoprecipitation. A mouse anti-FLAG antibody (5µg, Cat. No 8146, Cell Signaling Technology, Danvers, MA, USA) was added to the sample and incubated for 1 h at 4 °C on a rotating platform. The complex was then incubated with Protein A/G PLUS-Agarose beads (Cat. No 2003, Santa Cruz Biotechnology, Dallas, Texas, USA) for 1 additional hour at 4 °C on a rotating platform. The complex was subsequently washed 3–4 times in washing buffer, and elution was performed with 2x Laemmli buffer. After centrifugation, the supernatant was removed and loaded onto a Tris glycine 4–10 % SDS-PAGE gel (100 V, 2 h), before transfer onto nitrocellulose membranes (100 V, 90 min). Protein immunodetection on membranes was assessed by using overnight at 4 °C a rabbit anti-HA antibody (dilution 1:1000) against the HA-tagged Arrestins. The primary antibody was detected using a secondary anti-rabbit IgG HRP-linked antibody (dilution 1:1000) for 1 h and the membranes were developed with Amersham ECL Plus chemiluminescent detection (Cat. No RPN2232, GE Healthcare, Little Chalfont, UK) and images were acquired using the ImageQuant LAS4000 system (GE Healthcare, Little Chalfont, UK). For Co-IP experiments with the FLAG-V_2R receptor, cells were treated with vehicle or Vasopressin (AVP, 100 nM, Cat. No AS-24289, Eurogentec, Seraing, Belgium) for 10 min before lysis.

2.11. DATA ANALYSIS

Data were analyzed using GraphPad Prism v.6 (GraphPad Software, San Diego, CA, USA), Microsoft Excel [Microsoft Office, Microsoft®, USA, version 16.16.24 (200713)] and ImageJ v.1.47 (National Institute of Health, USA) bundled with Java 1.8.0_172. JACop plugin for Image J was used to calculate the Pearson's correlation coefficient and the Van Steensel's cross correlation function (CCF) and to analyze images for the colocalization experiments. The Pearson's correlation coefficient provides information on the intensity distribution within the colocalizing region. Pearson's coefficients range from +1 to −1, with +1 representing a positive correlation (colocalization), −1 representing a negative correlation (exclusion), and 0 representing no relationship. Values from 0 to 0.1: No colocalization; From 0.1 to 0.3: Weak colocalization; From 0.3 to 0.5: Medium colocalization; From 0.5 to +1: Strong colocalization.

The Van Steensel's CCF shows how the Pearson's coefficient changes after shifting the red image voxels over the green image. The Pearson's coefficient is then plotted as the function of pixelshift (δ). By observing the shape of this cross-correlation function (CCF) plot as function of this shift, it can be determined if the signals of the two channels are actually positively correlated (peak at the

Published in : Biochemical Pharmacology (2024), vol. 220, 116013
DOI: 10.1016/j.bcp.2023.116013
Status : Postprint (Author's version)

center), mutually exclude each other (dip at the center), or simply overlap randomly (no features visible). Statistical analysis was performed with statistical significance determined at the following levels: not significant: $p > 0.05$; significant: $p < 0.05$. If the data followed a Gaussian distribution, we compared them using unpaired *t*-test. However, if the normal distribution of data or the homogeneity of their standard deviation was not verified, we compared them using the nonparametric Mann-Whitney *U* test.

3. Results

3.1. GPR101 CONSTITUTIVELY RECRUITS ARRESTIN 2 AND ARRESTIN 3

Previous investigations have established that GPR101 constitutively activates several G protein-dependent pathways[37]. However, a comprehensive profiling of its interaction with transducers has not been reported. Thus, we established a fingerprint of GPR101 interacting partners with our previously described Nanoluciferase (NLuc) complementation assay[38]. It consists in splitting the NLuc in two parts, a small 13 amino acid peptide fused with the receptor C-terminus with a spacer and the large moiety (LgBiT) fused with G proteins or arrestins. We could confirm a constitutive interaction of the receptor with G_s, G_q, G_{11}, G_{12} and G_{13} (Fig. 1A). In addition, we detected a previously unreported constitutive recruitment of Arrestin 3 (Fig. 1A).

Published in : Biochemical Pharmacology (2024), vol. 220, 116013
DOI: 10.1016/j.bcp.2023.116013
Status : Postprint (Author's version)

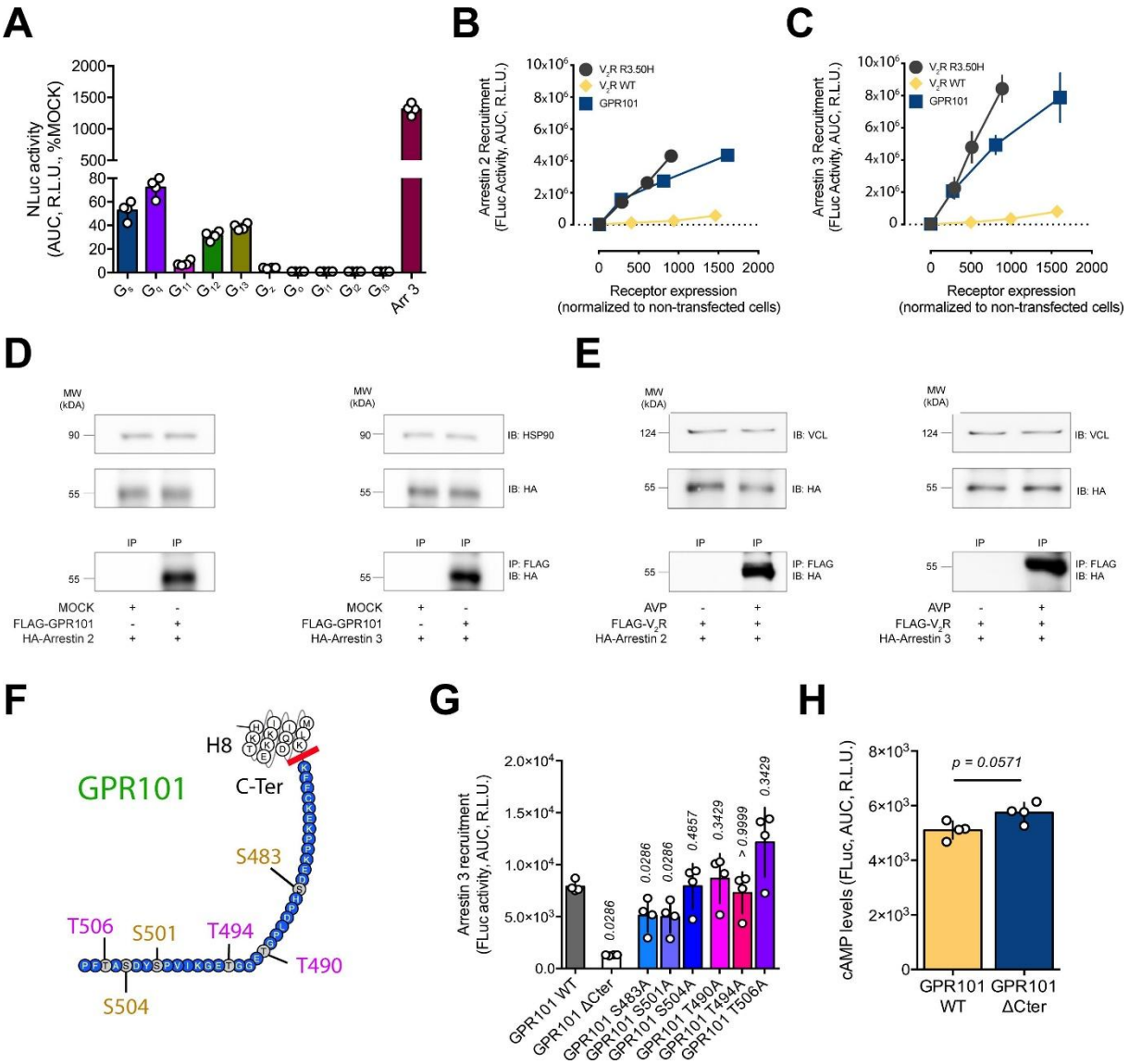

Fig. 1. GPR101 constitutively recruits arrestin 2 and arrestin 3. A-B. Constitutive recruitment of different transducers (G_s, G_q, G_{11}, G_{12}, G_{13}, G_z, G_o, G_{i1}, G_{i2}, G_{i3} and Arrestin 3) by GPR101-NP measured with a nanoluciferase (NLuc) complementation assay. **A.** The results are represented as a percentage of MOCK-transfected cells. n = 4 independent experiments. **B**-**C.** Constitutive recruitment of Arrestin 2 (**B**) and Arrestin 3 (**C**) by increasing concentrations of GPR101 (0, 7.5, 15 and 30 µg), measured with a firefly luciferase (FLuc) complementation assay. The expression levels following transfection of identical amounts of plasmids were determined experimentally by Flow cytometry. The receptors V_2R and V_2R R3.50H were used as negative and positive control, respectively. n = 6 independent experiments. **D.** Co-immunoprecipitation of FLAG-GPR101 (or MOCK) with anti-FLAG beads followed by immunodetection of HA-tagged Arrestin 2 or Arrestin 3 with anti-HA antibody on WB membranes. HSP90 (90 kDa) was used as the housekeeping protein for WB. Shown are representative pictures of three independent experiments. **E.** Co-immunoprecipitation of the non-constitutively active receptor FLAG-V_2R with HA-tagged Arrestin 2 or Arrestin 3. FLAG-V_2R-transfected cells were stimulated with AVP (100 nM) or vehicle for 10 min at 37 °C. The housekeeping protein VCL (124 kDa) was used as a loading control for WB. Shown are representative pictures of three independent experiments. **F.** Description of the GPR101 C-terminal tail (from to K471 to P508) as predicted by the GPCRdb (https://www.GPCRdb.org). The different point mutations of Ser/Thr residues are indicated. **G.** Arrestin 3

Published in : Biochemical Pharmacology (2024), vol. 220, 116013
DOI: 10.1016/j.bcp.2023.116013
Status : Postprint (Author's version)

recruitment mediated by GPR101 WT and mutants (△Cter, S483A, S501A, S504A, T490A, T494A and T506A) was measured with a FLuc complementation assay. *p* values were calculated by comparing each mutant with the WT receptor. n = 4 independent experiments. **H.** cAMP levels recorded after transient transfection of GPR101 WT or △Cter (15 µg) in HEK293 cells. *p* value was calculated by comparing cAMP levels of △Cter mutant to those of the WT receptor. n = 4 independent experiments. All data are Mean ± S.D. Arr 3: Arrestin 3; AUC: Area under curve; AVP: Vasopressin; C-Ter: C-terminus domain; H8: Helix 8; HSP 90: Heat shock protein 90; IB: antibody used for blotted membrane; IP: immunoprecipitated fraction; MW: Molecular weight; R.L.U: Relative luminescence unit; S: Serine; T: Threonine; VCL: Vinculin; WT: Wild-type. For statistical analysis of all data, *p* values were calculated using a two-sided Mann-Whitney *U* test and are indicated in the graphs. For statistical significance, the following limits were set: $p > 0.05$: not significantly different; $p < 0.05$: statistically significant.

To further document the interaction between GPR101 and arrestins, we first resorted to an in-house bioluminescent complementation assay based on the split of firefly luciferase (FLuc) to monitor GPR101-arrestin interaction in living cells[34], [42]. We fused the C-terminal part of FLuc to GPR101 C-terminus (to obtain GPR101-LFc) and the N-terminal part of FLuc to the N-terminal side of Arrestin 2 or 3 (FnL-Arr). We observed that in the presence of increasing amount of GPR101 expression, the Arrestin 2 and Arrestin 3-dependent luciferase signal was increased (Fig. 1B and C). V_2R, a typical class B strong binder of Arrestin 2 and 3 devoid of significant constitutive activity[15], [34], [43], was used as a negative control (Fig. 1B and C). To estimate the level of GPR101 constitutive activity in the arrestin pathway, we compared with the V_2R R3.50H mutant (designation of residues follows the Ballesteros and Weinstein system[44]), which is referred to as a receptor with high constitutive arrestin recruitment[43]. Although the activities cannot be compared directly as the levels of expression were different, we observed that the level of GPR101-mediated Arrestin 2 and 3 recruitment was in a similar range than that of V_2R R3.50H (Fig. 1B and C). To further confirm these observations, we examined the ability of GPR101 to co-immunoprecipitate with arrestins. Human embryonic kidney 293 (HEK293) cells were transiently transfected with GPR101 fused with a N-terminal FLAG epitope (FLAG-GPR101) and arrestin fused with a hemagglutinin (HA) tag. The cell lysates were treated with beads coated with an anti-FLAG antibody. The observed co-immunoprecipitation (co-IP) revealed by an anti-HA western blot (WB) confirmed the formation of a constitutive receptor-arrestin complex (Fig. 1D). As a comparison, the V_2R was co-immunoprecipitated with Arrestin 2 and Arrestin 3 following stimulation for 10 min at 37 °C with the agonist Vasopressin (AVP, 100 nM) or vehicle (Fig. 1E). Interestingly, unstimulated GPR101 formed similar levels of Arrestin complex compared to activated V_2R.

Next, we sought to detail the mode of association between GPR101 and arrestins. We generated a receptor mutant devoid of its C-terminal tail (GPR101 ΔCter, Fig. 1F), which is one of the canonical GPCR anchor domains for arrestins[45], [46]. We observed in our FLuc complementation assay that GPR101 ΔCter mutant had a drastically reduced recruitment of Arrestin 3 compared to wild-type (WT) receptor (Fig. 1G, $p = 0.0286$). Importantly, the constitutive increase of cAMP levels, measured with a Glo sensor system[40], was similar in GPR101 WT and GPR101 ΔCter ($p = 0.0571$). This result demonstrates that the GPR101 ΔCter constitutive activity is preserved and that the mutant has lost its ability to interact with Arrestin 3 (Fig. 1H). Arrestin affinity for receptor C-tail increases with the presence of phosphorylated serine (Ser or S) or threonine (Thr or T)[45]. The GPR101 C-terminus comprises 3 Ser (S483, S501 and S504) and 3 Thr (T490, T494 and T506) (Fig. 1F, source: GPCRdb).

Published in : Biochemical Pharmacology (2024), vol. 220, 116013
DOI: 10.1016/j.bcp.2023.116013
Status : Postprint (Author's version)

Thus, to identify the key residues essential for the association of the active receptor with Arrestin 3, we replaced with an alanine (Ala or A) each of these putative Ser/Thr phosphorylation sites present on GPR101 C-terminal tail (Fig. 1G). The serines S483 and S501 seemed to play a more critical role in the interaction with Arrestin 3 as their recruitment was significantly lower ($p = 0.0286$ for both mutants compared to WT receptor). None of the other mutants tested affected significantly Arrestin 3 recruitment. These data suggest that the interaction between arrestins and GPR101 necessitates prior phosphorylation of the C-tail, a classical feature for a GPCR[46].

3.2. ARRESTIN BINDING TO GPR101 LEADS TO CONSTITUTIVE INTERNALIZATION

Given the canonical function of arrestins in GPCR desensitization and internalization, we reasoned that the constitutive recruitment of arrestins by GPR101 could have an impact on the receptor cellular distribution. Therefore, we transfected HEK293 cells with the FLAG-GPR101 and first analyzed the receptor localization by confocal microscopy. These experiments revealed that, although the receptor was present at the cell surface membrane (labeled with wheat germ agglutinin, WGA) (Fig. 2A, upper panel, non-permeabilized cells), a substantial proportion of the fluorescent signal was located in intracellular endosome-like vesicles (Fig. 2A, lower panel, permeabilized cells), suggesting that GPR101 is internalized from the cell surface into the cytoplasm with a punctate distribution. In order to quantify these observations, we determined the total and cell surface expression levels of FLAG-GPR101 by flow cytometry (Fig. 2B). About 28 % of cells expressing FLAG-GPR101 on the cell surface exhibited 1.58-fold more fluorescence than the negative control (MOCK) (Fig. 2B, left panel, non-permeabilized cells). However, total expression levels of FLAG-GPR101 corresponded to 5.60-fold increase in fluorescence in comparison with MOCK-expressing cells (Fig. 2B, right panel, permeabilized cells). To specifically examine the GPR101 internalization dynamics, we performed anti-FLAG antibody feeding experiments (Fig. 2C). In this experiment, cell surface-expressed receptors were fed with a primary anti-FLAG antibody and detected using a secondary antibody conjugated to Alexa Fluor 488 (AF488) by flow cytometry. At 4 °C, a temperature known to block endocytosis, the primary anti-FLAG antibody labeled all the surface FLAG-GPR101 receptors (100 %). Then, when cells were incubated at 37 °C, the percentage of cell surface receptors decreased over time (Fig. 2C). These results show that following primary antibody labeling, incubation at 37 °C for 5 min was sufficient to induce significant constitutive endocytosis of GPR101. At the end of the incubation period (75 min), the immunoreactivity at the cell membrane was significantly reduced to 47.40 ± 5.13 % ($p = 0.0079$ for FLAG-GPR101 surface expression at 37 °C compared with 4 °C) (Fig. 2C) and had been transferred to the intracellular compartment. As a control, FLAG-tagged β_2AR was also tested. β_2AR is a well-characterized receptor known to internalize[47] mainly upon agonist stimulation. Here, we stimulated the receptor for 15 min at 37 °C with Isoproterenol (ISO), a reference agonist (Fig. 2D). After washing out the ligand, the receptor was allowed to recover at the cell surface and the percentage of expression significantly increased over time to reach 79.80±3.11 % at 75 min ($p = 0.0159$ for FLAG-β_2AR surface expression at 37 °C compared with 4 °C). Correspondingly, FLAG-β_2AR showed no internalization and recycling when stimulated with the vehicle alone at 4 °C or 37 °C (Fig. 2D). To causally link the observed internalization with arrestin action, we transfected HEK293 cells with FLAG-GPR101 and Arrestin 3

Published in : Biochemical Pharmacology (2024), vol. 220, 116013
DOI: 10.1016/j.bcp.2023.116013
Status : Postprint (Author's version)

fused to the green fluorescent protein (Arrestin 3-GFP). Cells co-expressing FLAG-GPR101 and Arrestin 3-GFP exhibited a significant colocalization within intracellular compartments under basal conditions, indicative of constitutive interaction (Fig. 2E).

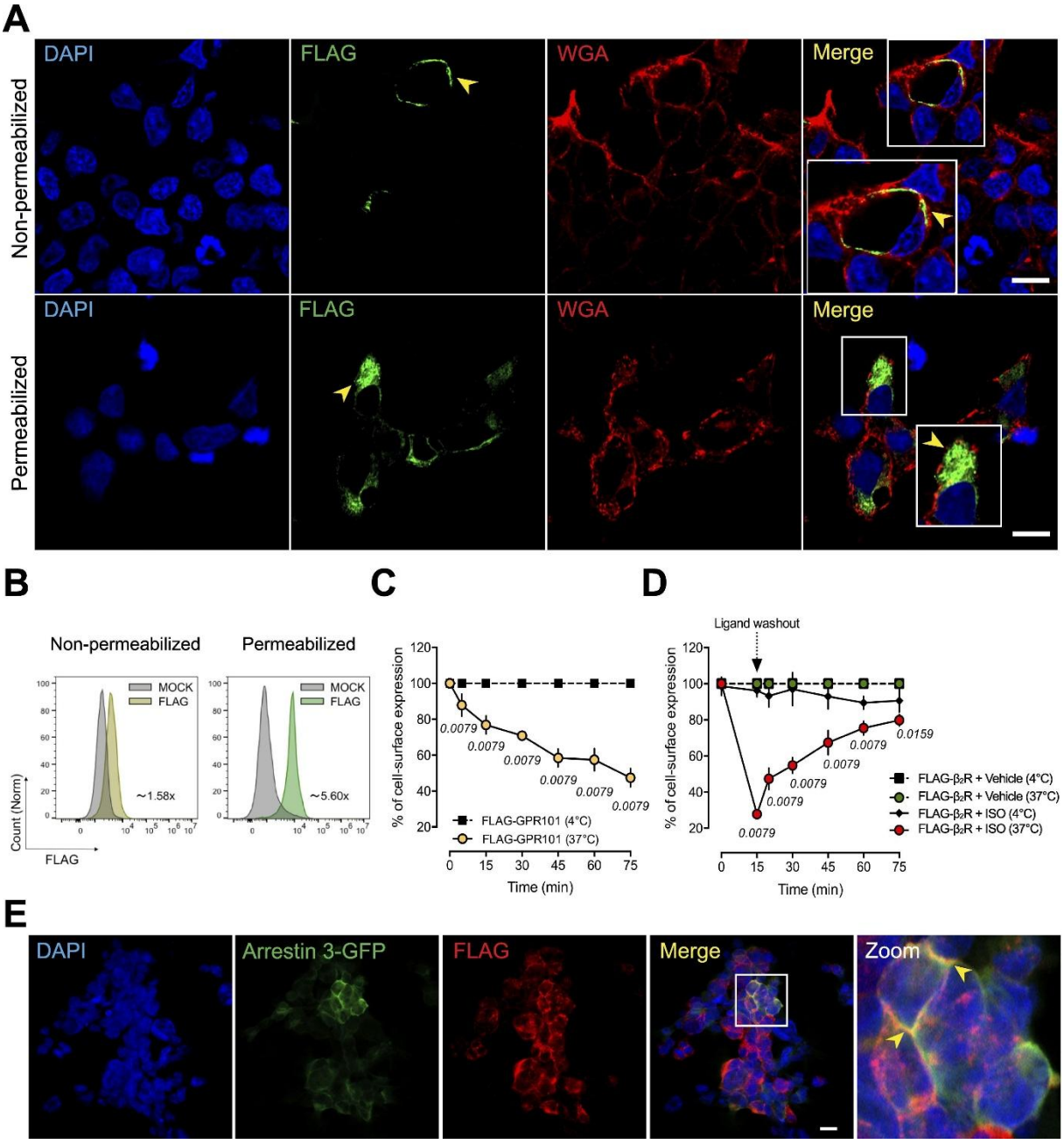

Fig. 2. GPR101 cellular distribution. A. Cells were transiently transfected with a FLAG-tagged human GPR101 receptor, fixed in 4 % PFA and stained with an anti-FLAG antibody (in green). The nucleus is stained with DAPI and appears in blue. The plasma membrane is stained with wheat germ agglutinin (WGA, in red). Upper panel: The cell surface receptor was labeled with a mouse anti-FLAG and an anti-mouse antibody conjugated to AF488 by using the non-permeabilized protocol (without detergent). Lower panel: Mild detergent (saponin) was added to the buffer to permeabilize the membrane and allow intracellular labeling of the receptor. Shown are representative images of three independent experiments. Insets show high magnification of the regions indicated by white rectangles and yellow arrows indicate FLAG-GPR101 location. Scale bar: 10 µm (×60

Published in : Biochemical Pharmacology (2024), vol. 220, 116013
DOI: 10.1016/j.bcp.2023.116013
Status : Postprint (Author's version)

magnification). **B.** HEK293 cells were transfected with MOCK or FLAG-GPR101 plasmid. Cell surface (left panel) and total receptor (right panel) expression was determined by using a primary anti-FLAG and a secondary AF488-conjugated anti-mouse antibody and analyzed by flow cytometry. The histograms of FLAG-GPR101-transfected cells (green) were overlaid with those of MOCK-transfected cells (grey). The *x* axis indicates the fluorescence intensity in a logarithmic scale and the *y* axis indicates the normalized cell number (count). n = 3 independent experiments. **C.** Internalization properties of GPR101 estimated by antibody feeding experiments were performed with the anti-FLAG antibody. HEK293 cells were transfected with FLAG-GPR101 WT plasmid. 48 h later, surface receptors were prelabeled with an anti-FLAG at 4 °C and excess of antibody was removed by several washing steps. After washing, cells were then incubated at 37 °C to allow internalization. Cell surface receptors were detected by anti-mouse antibody coupled to AF488 at different time-points (0, 5, 15, 30, 45, 60 and 75 min). 100 % represents the percentage of receptors present at the surface at 4 °C. n = 5 separate experiments. For each time-point, *p* values were calculated by comparing the cell surface expression of FLAG-GPR101 at 37 °C with its expression at 4 °C. **D.** Cell surface FLAG-tagged ß$_2$AR were treated with vehicle or isoproterenol (ISO, 10 µM) and measured with antibody labeling and flow cytometry. n = 5 independent experiments. For each time-point, *p* values were calculated by comparing the two groups, FLAG- ß$_2$AR stimulated with vehicle (at 37 °C) and FLAG- ß$_2$AR stimulated with ISO (at 37 °C). **E.** HEK293 cells were cultured on poly-D-lysine coated coverslips and transfected with FLAG-GPR101 and Arrestin 3-GFP plasmids. Cells were washed, fixed and imaged using a confocal microscope (FLAG-GPR101: Red; Arrestin 3-GFP: Green; DAPI: Blue). Representative images of experiments performed at least three times are shown. The arrows indicate representative colocalization signals. Scale bar: 10 µm (×60 magnification). The enlarged image of the selected area (rectangle) is shown in the fifth column (zoom). All data are Mean ± S.D. For statistical analysis of all data, *p* values were calculated using a two-sided Mann-Whitney *U* test and are indicated in the graphs. For statistical significance, the following limits were set: $p > 0.05$: not significantly different; $p < 0.05$: statistically significant. (For interpretation of the references to colour in this figure legend, the reader is referred to the web version of this article.)

Next, we determined by confocal microscopy the cellular distribution of the GPR101 ΔCter mutant, that possesses a N-terminal FLAG-tag. In stark contrast with what we observed in WT receptors (Fig. 2A and B), we noticed a markedly reduced FLAG signal inside the cell with a clustering of the receptor at the cell membrane in permeabilized cells (Fig. 3A, lower panel). The overall intensity and distribution of the signal in these cells was comparable to non-permeabilized cells prepared in parallel (Fig. 3A, upper panel). These results suggest that the C-terminus domain of GPR101 is involved in the internalization of the receptor. To demonstrate the arrestin implication in the internalization of GPR101, we repeated these experiments with WT FLAG-GPR101 transfected in cells genetically engineered by clustered regularly interspaced short palindromic repeats/CRISPR-associated protein 9 (CRISPR/Cas9) to lack both Arrestin 2 and 3 (HEK293 △Arrestin 2/3)[46], [47]. Like what was observed with the GPR101 △Cter mutant, we were unable to evidence by confocal microscopy the presence of the receptor in the intracellular compartment (Fig. 3B). We attributed the restricted expression of the receptor at the cell membrane of HEK293 △Arrestin 2/3 to the lack of Arrestin 2 and 3 in these cells. We quantified these observations for FLAG-GPR101 △Cter expression by FACS and could see an increase of 3.15-fold in fluorescence at the surface (77.20 % of positive in non-permeabilized cells) in comparison to the MOCK condition (Fig. 3C, left panel). We also observed an increase of 4.08-fold in fluorescence for FLAG-GPR101 △Cter total expression in the permeabilized cells (Fig. 3C, right panel). The FLAG-GPR101 △Cter mutant showed about 3-fold

Published in : Biochemical Pharmacology (2024), vol. 220, 116013
DOI: 10.1016/j.bcp.2023.116013
Status : Postprint (Author's version)

increase of surface expression compared to WT receptor (Fig. 3D, left panel). However, the total expression levels of both constructs appeared to be similar (Fig. 3D, right panel). Feeding experiments were repeated on the HEK293 △Arrestin 2/3 transfected with WT FLAG-GPR101. The internalization of FLAG-GPR101 in HEK293 △Arrestin 2/3 monitored at 37 °C was negligible compared to the HEK293 WT transfected with the same conditions (Fig. 3E).

Published in : Biochemical Pharmacology (2024), vol. 220, 116013
DOI: 10.1016/j.bcp.2023.116013
Status : Postprint (Author's version)

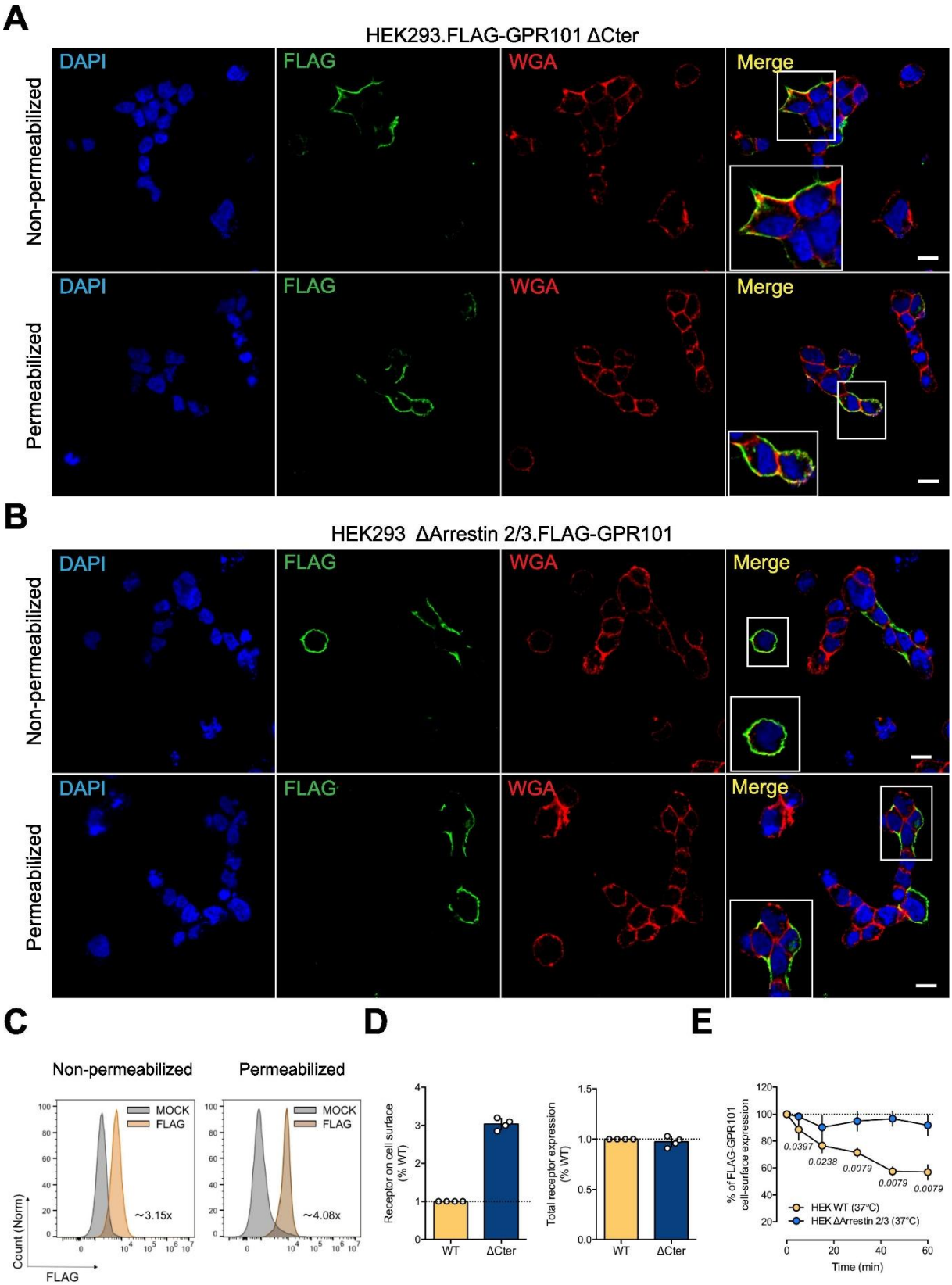

Fig. 3. Constitutive GPR101 internalization is mediated by arrestins. A. HEK293 cells transiently transfected with FLAG-GPR101 ΔCter and labeled (in green) with (upper panel) or without (lower panel) permeabilization were imaged by confocal microscopy. The nucleus is stained with DAPI (blue) and the plasma membrane is

Published in : Biochemical Pharmacology (2024), vol. 220, 116013
DOI: 10.1016/j.bcp.2023.116013
Status : Postprint (Author's version)

labeled with wheat germ agglutinin (WGA, red). Representative images of experiments performed at least three times are shown. Scale bar: 10 µm (×60 magnification). **B.** HEK293 △Arrestin 2/3 were transiently transfected with WT FLAG-GPR101. Cells were labeled with (upper panel) or without (lower panel) permeabilization. Representative images of experiments performed at least three times are shown. Scale bar: 10 µm (×60 magnification). **C.** Cell surface and total expression of FLAG-GPR101 △Cter was performed by flow cytometry. The histograms of FLAG-GPR101 △Cter-transfected cells (brown) were overlaid with those of MOCK-transfected cells (grey). The *x* axis indicates the fluorescence intensity in a logarithmic scale and the *y* axis indicates the normalized cell number (count). n = 6 independent experiments. **D.** Quantification of surface (left panel) and total (right panel) FLAG-GPR101 signals. The quantified FLAG-GPR101 △Cter signal was normalized to that of FLAG-GPR101 WT. n = 4 independent experiments. **E.** △Arrestin 2/3 and WT HEK293 cells were transfected with FLAG-GPR101. After 48 h, surface receptors were prelabeled with an anti-FLAG antibody at 4 °C and allowed to internalize at various time points (0, 5, 15, 30 and 60 min) at 37 °C. Flow cytometry experiments were performed to detect the FLAG epitope tag introduced into the extracellular N-terminal domain of GPR101. 100 % represents the receptor present at the cell surface at 4 °C. n = 5 independent experiments. For each time-point, *p* values were determined by comparing the cell surface expression of FLAG-GPR101 in HEK293 WT and △Arrestin 2/3 cells at 37 °C. All data are Mean ± S.D. For statistical analysis of all data, *p* values were calculated using a two-sided Mann-Whitney *U* test and are indicated in the graphs. For statistical significance, the following limits were set: $p > 0.05$: not significantly different; $p < 0.05$: statistically significant. (For interpretation of the references to colour in this figure legend, the reader is referred to the web version of this article.)

3.3. GPR101 IS DISPATCHED TO EARLY ENDOSOMES THROUGH THE CLATHRIN PATHWAY

Next, we aimed at tracking the receptor intracellular trafficking and determine the nature of the intracellular vesicles where GPR101 was located. To find out which endocytosis pathway was responsible for GPR101 internalization, we first used clathrin as a marker for the clathrin-mediated pathway and caveolin-1 as a marker for the caveolin-mediated pathway[47], [48]. GPR101 was markedly colocalized with clathrin within the cells (Fig. 4A, Van steensel's cross correlation factor (CCF) peak at 0.573) but not with caveolin (Fig. 4B, weak colocalization with CCF peak at 0.202). Furthermore, we sought to dissect the endocytic mechanisms for GPR101 and estimated the degree of receptor internalization when the cells were treated with Pitstop 2 (inhibitor of clathrin-dependent endocytosis[48], [49]), dynasore (inhibitor of dynamin activity that is necessary for clathrin-mediated endocytosis[50]) and sucrose (inhibitor of clathrin-mediated endocytosis[51]) or transfected with Dynamin K44A[52], a dominant negative version of dynamin (Fig. 4C). As shown by confocal microscopy, the treatment by these inhibitors increased the expression of GPR101 at the cell membrane in comparison with controls (vehicle or MOCK-treated cells) (Fig. 4C). Taken together, these data suggest that the increase in the cell surface expression of GPR101 is attributable to the inhibition of clathrin and dynamin activity, which prevents endocytosis. We quantified these findings by FACS analysis and we detected a significant increase in cell surface expression of FLAG-GPR101 in cells treated with these endocytosis inhibitors (pitstop 2, dynasore, sucrose and Dyn K44A) compared with their respective controls (Fig. 4D). For instance, the fluorescence for FLAG-GPR101-expressing cells treated with dynasore showed a 4-fold increase compared with vehicle-

Published in : Biochemical Pharmacology (2024), vol. 220, 116013
DOI: 10.1016/j.bcp.2023.116013
Status : Postprint (Author's version)

treated cells (Fig. 4E). Next, to assess the impact of GPR101 localization on its signaling, we measured the impact of the inhibition of internalization on the cAMP levels. As shown in Fig. 4F, treatment of GPR101-transfected cells with various concentrations of dynasore increased cAMP production compared to the vehicle. Overall, our data indicate that GPR101 is internalized through a clathrin and dynamin-dependent process and that GPR101-mediated increase of cAMP takes place primarily at the plasma membrane. Importantly, we also evaluated the receptor presence in the nucleus or other organelles and uncovered an absence of localization in the nucleus and only weak or marginal colocalization with other organelles. GM130 was used for the Golgi apparatus (CCF peak at 0.283), Sec16B and Sec23A for the endoplasmic reticulum (ER) (CCF peak at 0.259 and 0.227) and A-kinase anchor protein (AKAP)-RFP for mitochondria (CCF peak at 0.240) (Fig. 5A – D).

Published in : Biochemical Pharmacology (2024), vol. 220, 116013
DOI: 10.1016/j.bcp.2023.116013
Status : Postprint (Author's version)

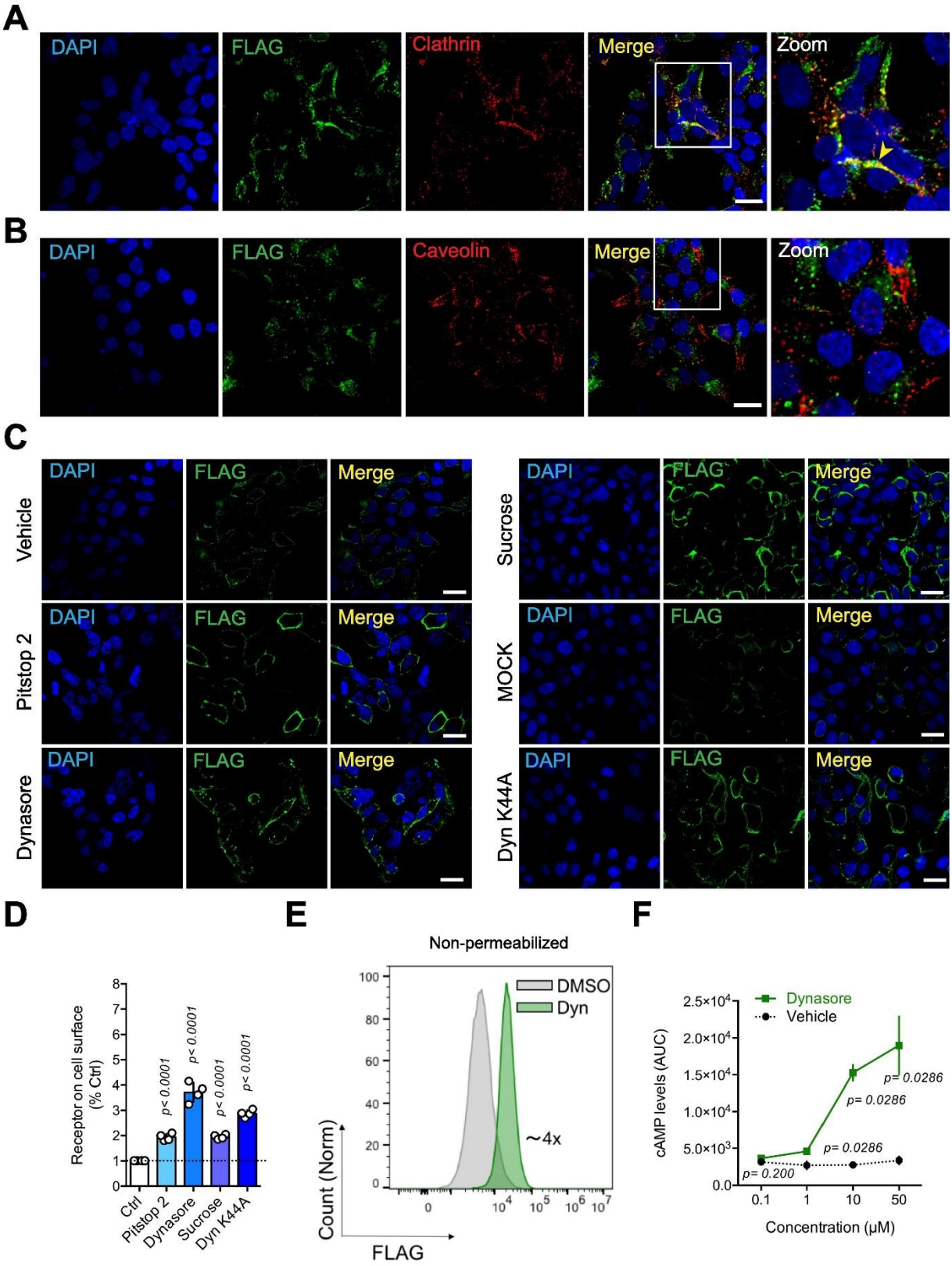

Fig. 4. GPR101 is internalized through a clathrin-dependent process. A-B. HEK293 cells were transiently transfected with FLAG-GPR101 and imaged by confocal microscopy following co-staining with an anti-FLAG (green) and anti-clathrin (red, **A**) or anti-caveolin (red, **B**) antibodies. Yellow arrows indicate representative colocalization signals. The enlarged images of the selected area (white rectangle) are shown in the fifth image

Published in : Biochemical Pharmacology (2024), vol. 220, 116013
DOI: 10.1016/j.bcp.2023.116013
Status : Postprint (Author's version)

(zoom). **C.** HEK293 cells expressing FLAG-GPR101 were subjected to treatment with vehicle (1 % DMSO), pitstop 2 (25 µM), dynasore (50 µM) and hyperosmotic sucrose (0.5 M) for 30 min at 37 °C. FLAG-GPR101-transfected HEK293 cells were also transfected with the dynamin K44A mutant (or MOCK). The immunofluorescent staining of FLAG-GPR101 was performed with the non-permeabilized protocol. Blue: DAPI; Green: FLAG-Gpr101. Representative images of experiments performed at least three times are shown. Scale bar: 10 µm (×60 magnification). **D.** Cell surface expression of FLAG-GPR101 was measured by flow cytometry. The histograms of FLAG-GPR101-transfected cells stimulated with 50 µM dynasore (Dyn, green) were overlaid with those treated with vehicle (1 % DMSO, grey) at 37 °C for 30 min. The *x* axis indicates the fluorescence intensity in a logarithmic scale and the *y* axis indicates the normalized cell number (count). n = 6 independent experiments. **E.** Quantification of surface FLAG-GPR101 signals after treatment by different endocytosis inhibitors (pitstop 2, dynasore, sucrose and Dyn K44A). The quantified FLAG-GPR101 signal of each inhibitor was normalized to that of the control (ctrl). n = 4 independent experiments. *p* values were calculated by comparing the cell surface expression of FLAG-GPR101 following the treatment by endocytosis inhibitors and their controls. **F.** cAMP levels recorded after treatment of FLAG-GPR101^{+} transfected HEK293 cells by different concentrations of dynasore (0.1, 1, 10 and 50 µM) or vehicle (DMSO). For each concentration, *p* value was calculated by comparing cAMP levels of dynasore to those of the vehicle. n = 4 independent experiments. All data are Mean ± S.D. AUC: Area under curve. For statistical analysis of all data, *p* values were calculated using a two-sided Mann-Whitney *U* test and are indicated in the graphs. For statistical significance, the following limits were set: $p > 0.05$: not significantly different; $p < 0.05$: statistically significant. (For interpretation of the references to colour in this figure legend, the reader is referred to the web version of this article.)

Published in : Biochemical Pharmacology (2024), vol. 220, 116013
DOI: 10.1016/j.bcp.2023.116013
Status : Postprint (Author's version)

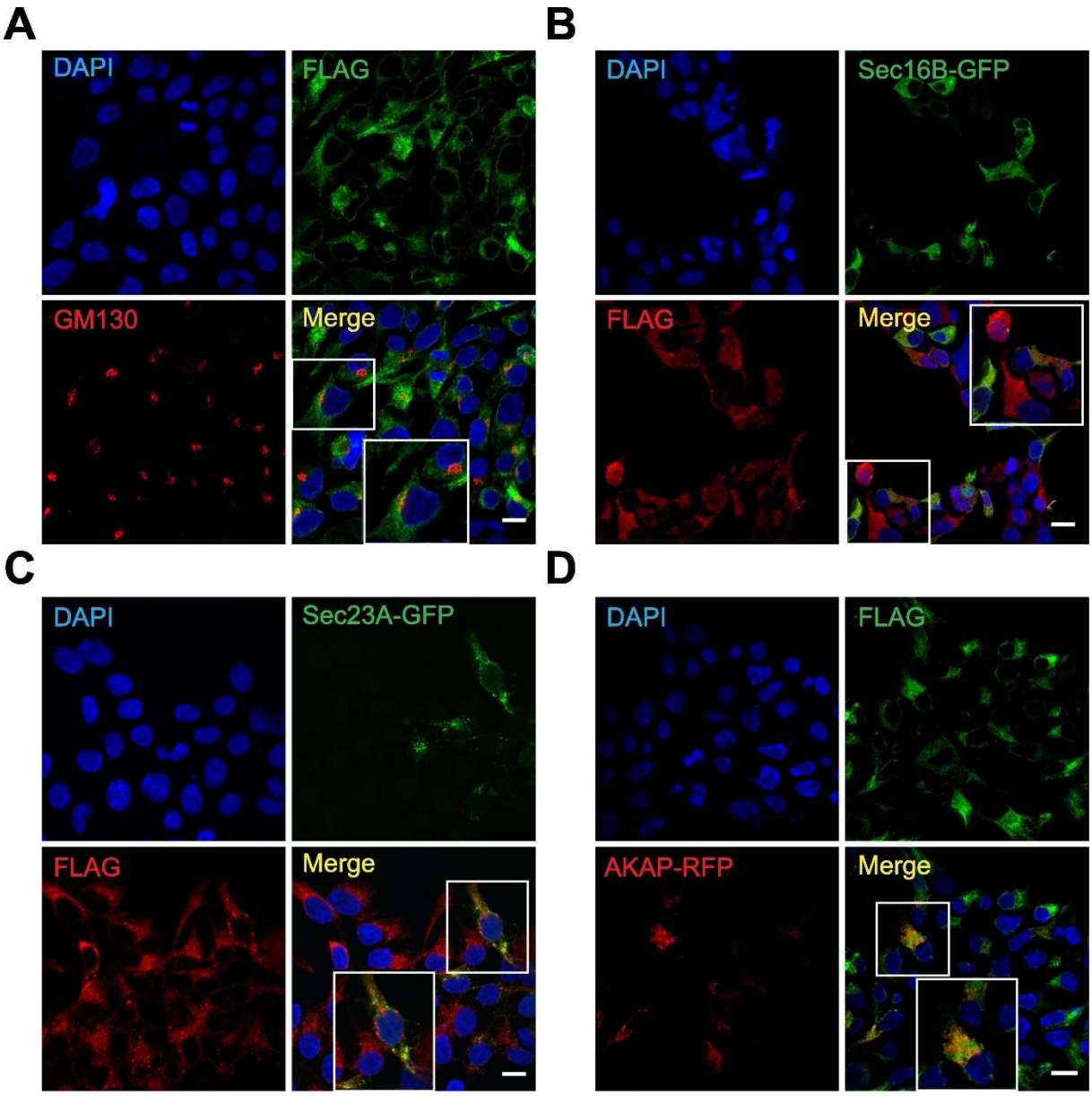

Fig. 5. GPR101 is not present in the Golgi apparatus, endoplasmic reticulum and mitochondria. A-D. Immunofluorescent co-staining of FLAG-GPR101 with **A**) GM130 (Golgi apparatus marker), **B**) Sec16B-GFP (endoplasmic reticulum marker), **C**) Sec23A-GFP (endoplasmic reticulum marker) and **D**) AKAP-RFP (mitochondria marker). DAPI is stained in blue. n = 3 separate experiments. Scale bar: 10 µm (×60 magnification). GFP: Green fluorescent protein; RFP: Red fluorescent protein. Insets show high magnification of the regions indicated by white rectangles. Scale bar: 10 µm (×60 magnification). (For interpretation of the references to colour in this figure legend, the reader is referred to the web version of this article.)

Next, we proceeded to further investigate the colocalization of GPR101 with different markers for endosomes, notably Rab proteins. Visual examination of the images suggests a prominent overlap of the internalized GPR101 with Rab5 as well as with early endosome antigen-1 (EEA-1), which suggests its presence in early endosomes (Fig. 6A and B). These findings were substantiated by quantification of the colocalization using the Pearson's coefficient (0.767 for Rab5 and 0.633 for EEA-1, both values greater than 0.5). Furthermore, by using JACoP plugin in ImageJ[53], [54], [55], we

Published in : Biochemical Pharmacology (2024), vol. 220, 116013
DOI: 10.1016/j.bcp.2023.116013
Status : Postprint (Author's version)

performed the Van Steensel's analysis and found that the CCF peaked at 0.767 (Rab5 colocalization) and 0.633 (EEA-1 colocalization) for constitutively internalized GPR101 and the bell-shaped curve was centered on the pixelshift (δ) = 0. Furthermore, the decrease in CCF with increasing X-axis offset between the two channels confirmed the specific overlay of the two signals. Through such analyses, these results show a positive correlation and a strong colocalization between GPR101 and Rab5 or EEA-1, indicating that after the internalization of GPR101, the vesicles are dispatched to early endosomes.

Published in : Biochemical Pharmacology (2024), vol. 220, 116013
DOI: 10.1016/j.bcp.2023.116013
Status : Postprint (Author's version)

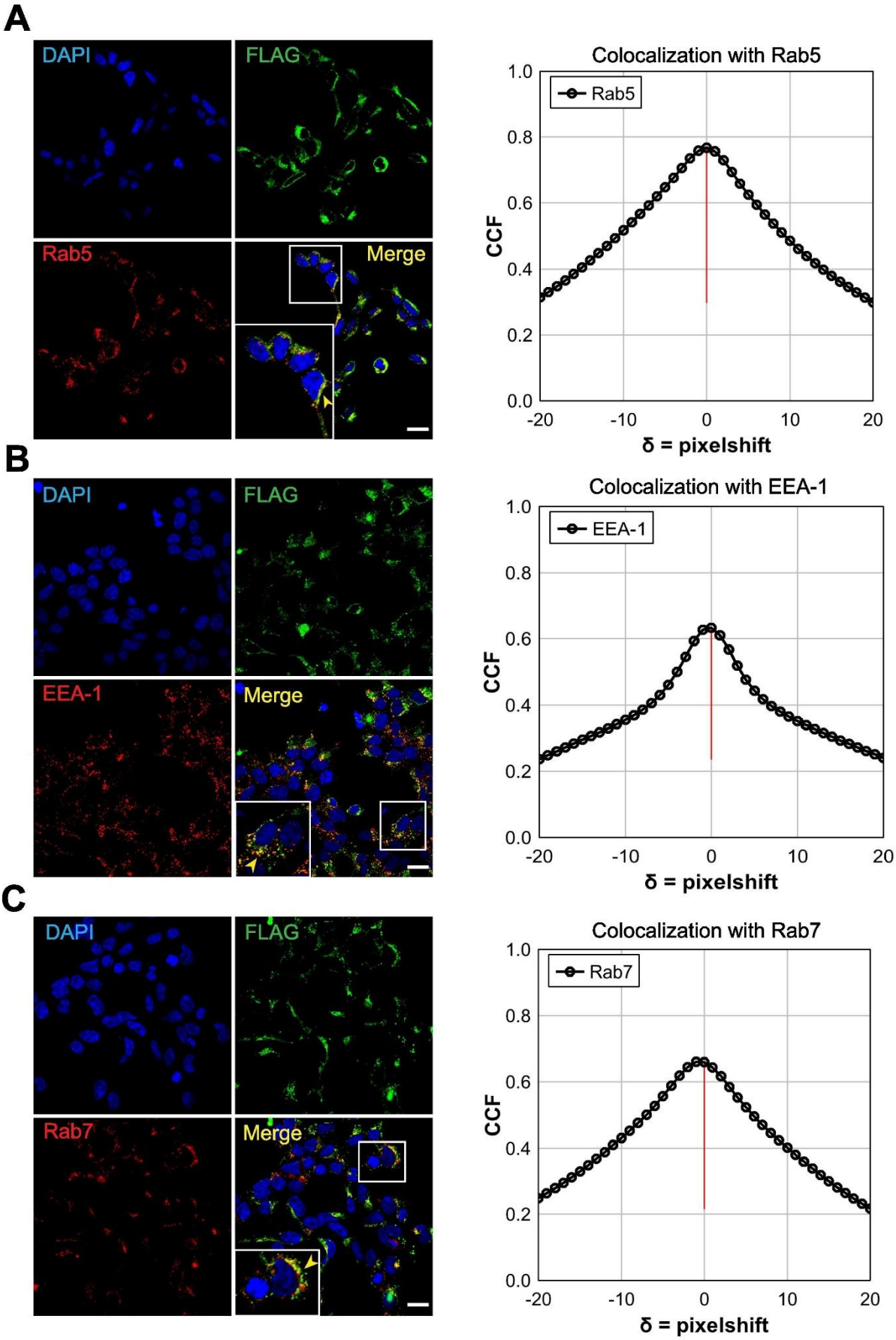

Published in : Biochemical Pharmacology (2024), vol. 220, 116013
DOI: 10.1016/j.bcp.2023.116013
Status : Postprint (Author's version)

Fig. 6. Internalized GPR101 is dispatched to early and late endosomes. A-C. Immunofluorescent co-staining of FLAG-GPR101 with Rab5 (early endosome marker, **A**), EEA-1 (early endosome marker, **B**) and Rab7 (late endosome marker, **C**). Blue: DAPI; Green: FLAG-GPR101; Red: Endosomal markers. In all images, insets show high magnification of the regions indicated by white rectangles. Yellow arrows indicate representative colocalization signals. Representative images from three independent experiments are shown. Scale bar: 10 µm (×60 magnification). Van Steensel's CCF analysis was performed by using the JACoP plugin in Image J and the cross correlation factor (CCF) is shown as function of the pixelshift (δ) for the colocalization of FLAG-GPR101 with Rab5, EEA-1 and Rab7, respectively. For the quantification, a total of n = 30 images from three independent experiments were used. (For interpretation of the references to colour in this figure legend, the reader is referred to the web version of this article.)

3.4. GPR101 IS MAINLY SORTED THROUGH THE LYSOSOMAL DEGRADATION PATHWAY

To establish the fate of the receptor, we performed the labeling of Rab7 and Rab11 together with FLAG-GPR101. We observed a marked overlap in localization between internalized GPR101 and Rab7 (Fig. 6C). The specificity of the colocalization was also confirmed using the Van Steensel's quantification analysis, which resulted in a CCF peak at 0.660. These results suggest that GPR101 is associated with Rab7 and sorted to late (or lysosomal) endosomes. However, only a negligible colocalization of internalized GPR101 with Rab11 was observed (CCF peak at 0.220) (Fig. 7A). Thus, GPR101 appeared to be primarily absent from the recycling endosomes. As a comparison, we analyzed the intracellular fate of the β_2AR upon agonist-induced endocytosis (following stimulation with 10 µM ISO). β_2AR is known to be sorted through recycling endosomes and was used as a positive control of this endosomal route[56]. The colocalization of β_2AR with the recycling marker Rab11 was confirmed by our experiment (Fig. 7B, CCF peak at 0.584).

Published in : Biochemical Pharmacology (2024), vol. 220, 116013
DOI: 10.1016/j.bcp.2023.116013
Status : Postprint (Author's version)

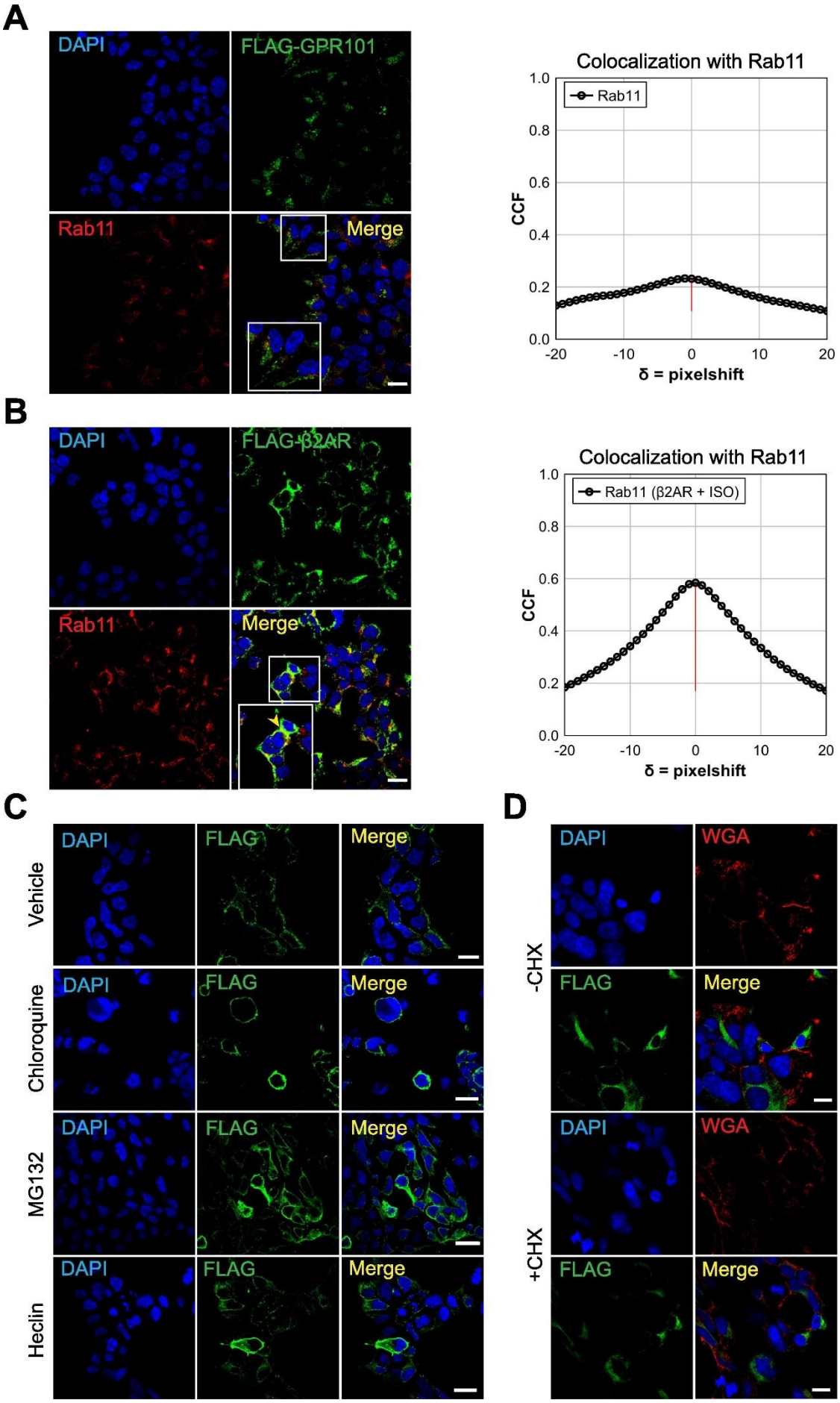

Published in : Biochemical Pharmacology (2024), vol. 220, 116013
DOI: 10.1016/j.bcp.2023.116013
Status : Postprint (Author's version)

Fig. 7. GPR101 is mainly sorted through the lysosomal degradation pathway and not recycled back to the membrane. A. Immunofluorescent co-staining of FLAG-GPR101 with Rab11 (recycling endosome marker). **B.** Colocalization studies of FLAG-ß2AR (stimulated with 10 µM of isoproterenol) and Rab11. Blue: DAPI; Green: FLAG; Red: Rab11. Insets show high magnification of the regions indicated by white rectangles. Yellow arrows indicate representative colocalization signals. Representative images from three independent experiments are shown. Scale bar: 10 µm (×60 magnification). Van Steensel's CCF analysis was performed by using the JACoP plugin in Image J and the cross correlation factor (CCF) is shown as function of the pixelshift for colocalization of FLAG-GPR101 or FLAG-ß2AR (stimulated with 10 µM of isoproterenol) with Rab11. For the quantification, a total of n = 30 images from three independent experiments were used. **C.** HEK293 cells expressing FLAG-GPR101 were subjected to treatment with vehicle (1 % DMSO), chloroquine (200 µM, 30 min), MG132 (10 µM, 2 h) and Heclin (10 µM, 2 h) at 37 °C. The immunofluorescent staining of FLAG-GPR101 was performed in the non-permeabilized protocol. Blue: DAPI; Green: FLAG-Gpr101. Representative images of experiments performed at least three times are shown. Scale bar: 10 µm (×60 magnification). **D.** FLAG-GPR101 transfected HEK293 cells were treated with cycloheximide (CHX, 10 µg ml^{-1}, 4 h). The immunofluorescent staining of FLAG-GPR101 and WGA was performed with the permeabilized protocol. Blue: DAPI; Green: FLAG-Gpr101; Red: WGA. Representative images of experiments performed at least three times are shown. Scale bar: 10 µm (×60 magnification). (For interpretation of the references to colour in this figure legend, the reader is referred to the web version of this article.)

To further confirm that GPR101 is sorted to lysosomal compartments, we pretreated FLAG-GPR101-transfected cells with chloroquine that blocks proteolytic enzymes by elevating the pH of lysosomes[57]. We observed that GPR101 expression was increased at the plasma membrane in chloroquine-treated cells, thus excluding the possibility that this receptor was not detected in lysosomes because it had been immediately degraded (preventing accumulation) (Fig. 7C). Furthermore, as ubiquitination is known to target many GPCRs for lysosomal or proteasomal degradation[58], we performed the same experiment by treating the cells with MG132 (proteasome and ubiquitination inhibitor[59]) or Heclin (a HECT E3 ubiquitin ligase inhibitor[60]). As shown in Fig. 7C, MG132 or Heclin increased the levels of GPR101 cell surface expression compared to the vehicle. Thus, after transiting in early endosomes, GPR101 is dispatched for the lysosomal degradation pathway and not recycled back to the membrane. To determine the intracellular origin (recycling vs newly synthesized receptors) of the receptors observed at the plasma membrane after internalization, we pretreated FLAG-GPR101-transfected cells for a period of 4 h with cycloheximide (CHX, a protein synthesis inhibitor[61]). We observed a significant loss of receptors at the cell surface (Fig. 7D) in CHX-treated cells compared to the vehicle control, suggesting that GPR101 is not recycled to the plasma membrane and that de novo synthesis plays a major role in the appearance of the receptor at the cell surface.

4. Discussion

In this report, we unveil the constitutive recruitment of arrestins to the orphan receptor GPR101 and describe how it impacts the receptor cellular location and trafficking. We found that GPR101 is constitutively internalized through the basal recruitment of Arrestin 2 and 3 in a clathrin-mediated manner. We identified the C-terminal tail of the receptor as critically involved in the interaction with

Published in : Biochemical Pharmacology (2024), vol. 220, 116013
DOI: 10.1016/j.bcp.2023.116013
Status : Postprint (Author's version)

arrestins and hence internalization. This mechanism involving arrestins and clathrin constitutively relocates the receptor principally to early endosomes and is then directed to the lysosomal pathway. Interestingly, other constitutively active orphan receptors have been reported to bind arrestins[62], [63].

Using a C-terminally truncated mutant of GPR101, we were able to show that the C-terminal residues of GPR101 are required for constitutive Arrestin 3 recruitment by GPR101 but not for G protein activation. This supports the general idea that membrane-distal parts of the GPCR C-tail are not always directly involved in efficient G protein coupling[64]. Structural and biophysical studies have demonstrated that the C-terminal tails of the family A, rhodopsin-like, GPCRs are functionally important for facilitating the association of the receptor with various cellular proteins (such as arrestins) and thereby regulating receptor desensitization, endocytosis, and intracellular signaling. Furthermore, truncation of the C-terminal tail resulted in a mutant that was almost exclusively present on the cell surface. This cell surface expression could largely be attributed to the lack of arrestin recruitment leading to the inhibition of internalization. Point mutations of Ser and Thr residues present in GPR101 C-tail resulted in mutants where the Arrestin 3 recruitment was only slightly affected compared to the WT receptors. Therefore, none of the phosphorylated residues is individually critical for the recruitment of arrestins. This is in line with published literature where the current paradigms, for example the Flute model, state that arrestins are able to recognize a wide range of phosphorylation patterns of GPCRs, contributing to their diverse functions[65]. Different patterns of phosphorylation have already been validated such as PX(X)PXXP (where P is the phosphorylated residue and X any amino acid)[66], [67] and more recently PXPP[68], [69]. Interestingly, GPR101 possesses a PX(X)PXXP motif (S501, S504 and T506) that may serve for arrestin binding and activation. Our findings suggest that the receptor presence at the membrane is highly regulated. Thus, it is tempting to speculate that GPR101 may function, at least in part, as a versatile signaling unit driving basal tone in various pathways to regulate physiological processes such as GH secretion. Interestingly, another constitutively active orphan GPCR, GPR3, has been recently proposed to be a regulator for brown adipose tissue function[70].

The process of internalization is a well-described phenomenon to desensitize most GPCRs[70]. It was initially thought that this mechanism was a way to mitigate over-activation of the receptor by extracellular ligands[71]. More recently, the signaling activity of receptor in intracellular compartment gained a growing interest[72], [73]. Over the years, it has become evident that GPCR signaling is much more complex than once believed. For most receptors, a variety of ligands and intracellular signaling pathways are available, and numerous regulatory mechanisms are thus required for obtaining specific biological responses. The process of receptor trafficking plays a critical role in regulating GPCR function by controlling the level of receptors in the cell membrane hence controlling the number of receptors that are available for activation of extracellular ligands. Receptor trafficking includes the maturation and insertion of newly synthesized receptors in the cell membrane as well as the internalization of receptors from the surface and the subsequent intracellular sorting.

Published in : Biochemical Pharmacology (2024), vol. 220, 116013
DOI: 10.1016/j.bcp.2023.116013
Status : Postprint (Author's version)

Here, we show that GPR101 is clustered mainly in early endosomes following internalization. Our results are in accordance with other studies reporting that in clathrin-mediated internalization, receptors are targeted to the early endosomes and are usually downregulated through an ubiquitin-dependent sorting process[74]. In contrast, the caveolin-dependent endocytosis leads mainly to rapid receptor turnover and recycling[75]. Although further studies in a more physiological context would shed more light on this, we cannot exclude at this stage that the constitutive internalization of GPR101 has some physiological importance besides desensitization. We may hypothesize that, given its high level of constitutive activity, the receptor presence at the cell surface should be tightly controlled. In this context, although we cannot completely exclude marginal contribution of the slow-recycling pathway, constitutive internalization and degradation would serve as a cellular mechanism to mitigate GPR101-mediated signaling tonus. Another GH secretagogue, ghrelin receptor, is known to constitutively internalize as an integral part of its cellular physiology, although it is recycled to the membrane under certain circumstances [76].

CRediT authorship contribution statement

Dayana Abboud: Conceptualization, Formal analysis, Investigation, Methodology, Visualization, Writing – original draft, Writing – review & editing, Data curation, Resources, Validation. **Clauda Abboud:** Formal analysis, Investigation, Validation, Visualization, Writing – review & editing, Data curation, Methodology, Resources. **Asuka Inoue:** Methodology, Resources, Writing – review & editing. **Jean-Claude Twizere:** Methodology, Resources, Writing – review & editing. **Julien Hanson:** Conceptualization, Data curation, Formal analysis, Funding acquisition, Investigation, Methodology, Project administration, Resources, Supervision, Validation, Visualization, Writing – original draft, Writing – review & editing.

Declaration of competing interest

The authors declare that they have no known competing financial interests or personal relationships that could have appeared to influence the work reported in this paper.

Acknowledgements

This work was supported by the Fonds pour la Recherche Scientifique (F.R.S.-FNRS, Belgium) Incentive Grant for Scientific Research (F.4510.14), Research Project (PDR T.0111.19 and T.0099.23), Research Credit (CDR J.0083.21), Télévie (7461117 F, 7454719 F), University of Liège, Fédération Wallonie-Bruxelles (Action de Recherche Concertée ARC 17/21-01, Belgium) and Léon Fredericq Foundation (Belgium). DA was supported by Wallonie-Bruxelles International (WBI.IN, Belgium) and Télévie postdoctoral fellowships (7461117 F and 7454719 F, Belgium). CA is supported by a Marie

Published in : Biochemical Pharmacology (2024), vol. 220, 116013
DOI: 10.1016/j.bcp.2023.116013
Status : Postprint (Author's version)

Sklodowska-Curie Action (MSCA 101109841, Horizon Europe) postdoctoral fellowship. JH and JCT are F.R.S.- FNRS Senior Research Associates. A.I. was funded by KAKENHI JP21H04791 and JP21H05113 from Japan Society for the Promotion of Science (JSPS); JPMJFR215T from Japan Science and Technology Agency (JST). JH, DA and CA are members of the "European Research Network on Signal Transduction" (ERNEST, COST action CA18133). We thank the GIGA imaging platform for the technical support in confocal image acquisition and flow cytometry analysis.

Data availability

Data will be made available on request.

References

[1] C. Laschet, N. Dupuis, J. Hanson, The G protein-coupled receptors deorphanization landscape, Biochem. Pharmacol. 153 (2018) 62–74.

[2] A.P. Davenport, S.P.H. Alexander, J.L. Sharman, A.J. Pawson, H.E. Benson, A.E. Monaghan, W.C. Liew, C.P. Mpamhanga, T.I. Bonner, R.R. Neubig, J.P. Pin, M. Spedding, A.J. Harmar, International Union of Basic and Clinical Pharmacology. LXXXVIII. G protein-coupled receptor list: recommendations for new pairings with cognate ligands, Pharmacol. Rev. 65 (2013) 967–986.

[3] K. Sriram, P.A. Insel, G Protein-Coupled Receptors as Targets for Approved Drugs: How Many Targets and How Many Drugs? Mol. Pharmacol. 93 (2018) 251–258.

[4] S.P. Alexander, A. Christopoulos, A.P. Davenport, E. Kelly, A. Mathie, J.A. Peters, E.L. Veale, J.F. Armstrong, E. Faccenda, S.D. Harding, A.J. Pawson, C. Southan, J. A. Davies, M.P. Abbracchio, W. Alexander, K. Al-Hosaini, M. Bäck, N.M. Barnes, R. Bathgate, J.-M. Beaulieu, K.E. Bernstein, B. Bettler, N.J.M. Birdsall, V. Blaho, F. Boulay, C. Bousquet, H. Bräuner-Osborne, G. Burnstock, G. Caló, J.P. Castaño, K.J. Catt, S. Ceruti, P. Chazot, N. Chiang, B. Chini, J. Chun, A. Cianciulli, O. Civelli, L.H. Clapp, R. Couture, Z. Csaba, C. Dahlgren, G. Dent, K.D. Singh, S.D. Douglas, P. Dournaud, S. Eguchi, E. Escher, E.J. Filardo, T. Fong, M. Fumagalli, R.R. Gainetdinov, M. de Gasparo, C. Gerard, M. Gershengorn, F. Gobeil, T.L. Goodfriend, C. Goudet, K.J. Gregory, A.L. Gundlach, J. Hamann, J. Hanson, R.L. Hauger, D.L. Hay, A. Heinemann, M.D. Hollenberg, N.D. Holliday, M. Horiuchi, D. Hoyer, L. Hunyady, A. Husain, A.P. IJzerman, T. Inagami, K.A. Jacobson, R.T. Jensen, R. Jockers, D. Jonnalagadda, S. Karnik, K. Kaupmann, J. Kemp, C. Kennedy, Y. Kihara, T. Kitazawa, P. Kozielewicz, H.-J. Kreienkamp, J.P. Kukkonen, T. Langenhan, K. Leach, D. Lecca, J.D. Lee, S.E. Leeman, J. Leprince, X.X. Li, T.L. Williams, S.J. Lolait, A. Lupp, R. Macrae, J. Maguire, J. Mazella, C.A. McArdle, S. Melmed, M.C. Michel, L.J. Miller, V. Mitolo, B. Mouillac, C.E. Müller, P. Murphy, J.-L. Nahon, T. Ngo, X. Norel, D. Nyimanu, A.-M. O'Carroll, S. Offermanns, M.A. Panaro, M. Parmentier, R.G. Pertwee, J.-P. Pin, E.R. Prossnitz, M. Quinn, R. Ramachandran, M. Ray, R.K. Reinscheid, P. Rondard, G.E. Rovati, C. Ruzza, G.J. Sanger, T. Schöneberg, G. Schulte, S. Schulz, D.L. Segaloff, C.N. Serhan, L.A. Stoddart, Y. Sugimoto, R.

Summers, V.P. Tan, D. Thal, W.W. Thomas, P.B.M.W.M. Timmermans, K. Tirupula, G. Tulipano, H. Unal, T. Unger, C. Valant, P. Vanderheyden, D. Vaudry, H. Vaudry, J.-P. Vilardaga, C.S. Walker, J.M. Wang, D.T. Ward, H.-J. Wester, G.B. Willars, T.M. Woodruff, C. Yao, R.D. Ye, THE CONCISE GUIDE TO PHARMACOLOGY 2021/22: G protein-coupled receptors, Br. J. Pharmacol. 178 Suppl 1 (2021) S27–S156.

[5] J.P. Mahoney, R.K. Sunahara, Mechanistic insights into GPCR-G protein interactions, Curr. Opin. Struct. Biol. 41 (2016) 247–254.

[6] N. Wettschureck, S. Offermanns, Mammalian G proteins and their cell type specific functions, Physiol. Rev. 85 (2005) 1159–1204.

[7] A. Patwardhan, N. Cheng, J. Trejo, Post-Translational Modifications of G Protein- Coupled Receptors Control Cellular Signaling Dynamics in Space and Time, Pharmacol. Rev. 73 (2021) 120–151.

[8] K. Eichel, M. von Zastrow, Subcellular Organization of GPCR Signaling, Trends Pharmacol. Sci. 39 (2018) 200–208.

[9] V.V. Gurevich, E.V. Gurevich, GPCR signaling regulation: The role of GRKs and arrestins, Front. Pharmacol. 10 (2019) 125.

[10] J.S. Gutkind, E. Kostenis, Arrestins as rheostats of GPCR signalling, Nat. Rev. Mol. Cell Biol. 19 (2018) 615–616.

[11] M. Grundmann, N. Merten, D. Malfacini, A. Inoue, P. Preis, K. Simon, N. Rüttiger, N. Ziegler, T. Benkel, N.K. Schmitt, S. Ishida, I. Müller, R. Reher, K. Kawakami, A. Inoue, U. Rick, T. Kühl, D. Imhof, J. Aoki, G.M. König, C. Hoffmann, J. Gomeza, J. Wess, E. Kostenis, Lack of beta-arrestin signaling in the absence of active G proteins, Nat. Commun. 9 (2018) 341.

[12] M. O'Hayre, K. Eichel, S. Avino, X. Zhao, D.J. Steffen, X. Feng, K. Kawakami, J. Aoki, K. Messer, R. Sunahara, A. Inoue, M. von Zastrow, J.S. Gutkind, Genetic evidence that beta-arrestins are dispensable for the initiation of beta(2)-adrenergic receptor signaling to ERK, Sci Signal. 10 (2017), https://doi.org/10.1126/scisignal.aal3395.

[13] E. Alvarez-Curto, A. Inoue, L. Jenkins, S.Z. Raihan, R. Prihandoko, A.B. Tobin, G. Milligan, Targeted Elimination of G Proteins and Arrestins Defines Their Specific Contributions to Both Intensity and Duration of G Protein-coupled Receptor Signaling, J. Biol. Chem. 291 (2016) 27147–27159.

[14] S.A. Laporte, R.H. Oakley, J.A. Holt, L.S. Barak, M.G. Caron, The interaction of beta-arrestin with the AP-2 adaptor is required for the clustering of beta 2-adrenergic receptor into clathrin-coated pits, J. Biol. Chem. 275 (2000) 23120–23126.

[15] R.H. Oakley, S.A. Laporte, J.A. Holt, M.G. Caron, L.S. Barak, Differential affinities of visual arrestin, beta arrestin1, and beta arrestin2 for G protein-coupled receptors delineate two major classes of receptors, J. Biol. Chem. 275 (2000) 17201–17210.

Published in : Biochemical Pharmacology (2024), vol. 220, 116013
DOI: 10.1016/j.bcp.2023.116013
Status : Postprint (Author's version)

[16] R.H. Oakley, S.A. Laporte, J.A. Holt, L.S. Barak, M.G. Caron, Molecular determinants underlying the formation of stable intracellular G protein-coupled receptor-beta-arrestin complexes after receptor endocytosis*, J. Biol. Chem. 276 (2001) 19452–19460.

[17] G.R. Pope, S. Tilve, C.A. McArdle, S.J. Lolait, A.-M. O'Carroll, Agonist-induced internalization and desensitization of the apelin receptor, Mol. Cell. Endocrinol. 437 (2016) 108–119.

[18] E.M. Smyth, S.C. Austin, M.P. Reilly, G.A. FitzGerald, Internalization and sequestration of the human prostacyclin receptor, J. Biol. Chem. 275 (2000) 32037–32045.

[19] M.M. Paing, A.B. Stutts, T.A. Kohout, R.J. Lefkowitz, J. Trejo, beta -Arrestins regulate protease-activated receptor-1 desensitization but not internalization or Down-regulation, J. Biol. Chem. 277 (2002) 1292–1300.

[20] F.F. Hamdan, M.D. Rochdi, B. Breton, D. Fessart, D.E. Michaud, P.G. Charest, S. A. Laporte, M. Bouvier, Unraveling G protein-coupled receptor endocytosis pathways using real-time monitoring of agonist-promoted interaction between beta-arrestins and AP-2, J. Biol. Chem. 282 (2007) 29089–29100.

[21] E.V. Moo, J.R. van Senten, H. Bräuner-Osborne, T.C. Møller, Arrestin-Dependent and -Independent Internalization of G Protein-Coupled Receptors: Methods, Mechanisms, and Implications on Cell Signaling, Mol. Pharmacol. 99 (2021) 242–255.

[22] S. Guo, X. Zhang, M. Zheng, X. Zhang, C. Min, Z. Wang, S.H. Cheon, M.-H. Oak, S.- Y. Nah, K.-M. Kim, Selectivity of commonly used inhibitors of clathrin-mediated and caveolae-dependent endocytosis of G protein-coupled receptors, Biochim. Biophys. Acta. 2015 (1848) 2101–2110.

[23] Y. Okamoto, H. Ninomiya, S. Miwa, T. Masaki, Cholesterol oxidation switches the internalization pathway of endothelin receptor type A from caveolae to clathrincoated pits in Chinese hamster ovary cells, J. Biol. Chem. 275 (2000) 6439–6446.

[24] B. Chini, M. Parenti, G-protein coupled receptors in lipid rafts and caveolae: how, when and why do they go there? J. Mol. Endocrinol. 32 (2004) 325–338.

[25] E. Boucrot, A.P.A. Ferreira, L. Almeida-Souza, S. Debard, Y. Vallis, G. Howard, L. Bertot, N. Sauvonnet, H.T. McMahon, Endophilin marks and controls a clathrinindependent endocytic pathway, Nature. 517 (2015) 460–465.

[26] J.C. Martinez-Morales, M.T. Romero-Avila, G. Reyes-Cruz, J.A. Garcia-Sainz, Roles of Receptor Phosphorylation and Rab Proteins in G Protein-Coupled Receptor Function and Trafficking, Mol Pharmacol. 101 (2022) 144–153.

[27] A.H. Hutagalung, P.J. Novick, Role of Rab GTPases in membrane traffic and cell physiology, Physiol. Rev. 91 (2011) 119–149.

[28] B. Bates, L. Zhang, S. Nawoschik, S. Kodangattil, E. Tseng, D. Kopsco, A. Kramer, Q. Shan, N. Taylor, J. Johnson, Y. Sun, H.M. Chen, M. Blatcher, J.E. Paulsen, M. H. Pausch, Characterization of Gpr101 expression and G-protein coupling selectivity, Brain Res. 1087 (2006) 1–14.

Published in : Biochemical Pharmacology (2024), vol. 220, 116013
DOI: 10.1016/j.bcp.2023.116013
Status : Postprint (Author's version)

[29] D. Abboud, A.F. Daly, N. Dupuis, M.A. Bahri, A. Inoue, A. Chevigne, F. Ectors, A. Plenevaux, B. Pirotte, A. Beckers, J. Hanson, GPR101 drives growth hormone hypersecretion and gigantism in mice via constitutive activation of G(s) and G(q/11), Nat Commun. 11 (2020) 4752.

[30] G. Trivellin, A.F. Daly, F.R. Faucz, B. Yuan, L. Rostomyan, D.O. Larco, M.H. Schernthaner-Reiter, E. Szarek, L.F. Leal, J.-H. Caberg, E. Castermans, C. Villa, A. Dimopoulos, P. Chittiboina, P. Xekouki, N. Shah, D. Metzger, P.A. Lysy, E. Ferrante, N. Strebkova, N. Mazerkina, M.C. Zatelli, M. Lodish, A. Horvath, R.B. de Alexandre, A.D. Manning, I. Levy, M.F. Keil, M. de la L. Sierra, L. Palmeira, W. Coppieters, M. Georges, L.A. Naves, M. Jamar, V. Bours, T.J. Wu, C.S. Choong, J. Bertherat, P. Chanson, P. Kamenický, W.E. Farrell, A. Barlier, M. Quezado, I. Bjelobaba, S.S. Stojilkovic, J. Wess, S. Costanzi, P. Liu, J.R. Lupski, A. Beckers, C.A. Stratakis, Gigantism and acromegaly due to Xq26 microduplications and GPR101 mutation, N. Engl. J. Med. 371 (2014) 2363–2374.

[31] D. Iacovazzo, R. Caswell, B. Bunce, S. Jose, B. Yuan, L.C. Hernández-Ramírez, S. Kapur, F. Caimari, J. Evanson, F. Ferraù, M.N. Dang, P. Gabrovska, S.J. Larkin, O. Ansorge, C. Rodd, M.L. Vance, C. Ramírez-Renteria, M. Mercado, A. P. Goldstone, M. Buchfelder, C.P. Burren, A. Gurlek, P. Dutta, C.S. Choong, T. Cheetham, G. Trivellin, C.A. Stratakis, M.-B. Lopes, A.B. Grossman, J. Trouillas, J.R. Lupski, S. Ellard, J.R. Sampson, F. Roncaroli, M. Korbonits, Germline or somatic GPR101 duplication leads to X-linked acrogigantism: a clinicopathological and genetic study, Acta Neuropathol Commun. 4 (2016) 56.

[32] A. Beckers, P. Petrossians, J. Hanson, A.F. Daly, The causes and consequences of pituitary gigantism, Nat. Rev. Endocrinol. 14 (2018) 705–720.

[33] H. Takakura, M. Hattori, M. Takeuchi, T. Ozawa, Visualization and quantitative analysis of G protein-coupled receptor-beta-arrestin interaction in single cells and specific organs of living mice using split luciferase complementation, ACS Chem Biol. 7 (2012) 901–910.

[34] N. Dupuis, C. Laschet, D. Franssen, M. Szpakowska, J. Gilissen, P. Geubelle, A. Soni, A.S. Parent, B. Pirotte, A. Chevigne, J.C. Twizere, J. Hanson, Activation of the Orphan G Protein-Coupled Receptor GPR27 by Surrogate Ligands Promotes beta-Arrestin 2 Recruitment, Mol Pharmacol. 91 (2017) 595–608.

[35] S.K. Shenoy, R.J. Lefkowitz, Receptor-specific ubiquitination of beta-arrestin directs assembly and targeting of seven-transmembrane receptor signalosomes, J. Biol. Chem. 280 (2005) 15315–15324.

[36] A. Budnik, K.J. Heesom, D.J. Stephens, Characterization of human Sec16B: indications of specialized, non-redundant functions, Sci. Rep. 1 (2011), https://doi.org/10.1038/srep00077.

[37] D.J. Stephens, N. Lin-Marq, A. Pagano, R. Pepperkok, J.P. Paccaud, COPI-coated ER-to-Golgi transport complexes segregate from COPII in close proximity to ER exit sites, J. Cell Sci. 113 (Pt 12) (2000) 2177–2185.

[38] C. Laschet, N. Dupuis, J. Hanson, A dynamic and screening-compatible nanoluciferase-based complementation assay enables profiling of individual GPCRG protein interactions, J. Biol. Chem. 294 (2019) 4079–4090.

Published in : Biochemical Pharmacology (2024), vol. 220, 116013
DOI: 10.1016/j.bcp.2023.116013
Status : Postprint (Author's version)

[39] C. Laschet, J. Hanson, Nanoluciferase-Based Complementation Assay to Detect GPCR-G Protein Interaction, Methods Mol. Biol. 2268 (2021) 149–157.

[40] J. Gilissen, P. Geubelle, N. Dupuis, C. Laschet, B. Pirotte, J. Hanson, Forskolin-free cAMP assay for Gi-coupled receptors, Biochem. Pharmacol. 98 (2015) 381–391.

[41] F. Fan, B.F. Binkowski, B.L. Butler, P.F. Stecha, M.K. Lewis, K.V. Wood, Novel genetically encoded biosensors using firefly luciferase, ACS Chem. Biol. 3 (2008) 346–351.

[42] P. Geubelle, J. Gilissen, S. Dilly, L. Poma, N. Dupuis, C. Laschet, D. Abboud, A. Inoue, F. Jouret, B. Pirotte, J. Hanson, Identification and pharmacological characterization of succinate receptor agonists, Br. J. Pharmacol. 174 (2017) 796–808.

[43] L.S. Barak, R.H. Oakley, S.A. Laporte, M.G. Caron, Constitutive arrestin-mediated desensitization of a human vasopressin receptor mutant associated with nephrogenic diabetes insipidus, Proc Natl Acad Sci U S a. 98 (2001) 93–98.

[44] J.A. Ballesteros, H. Weinstein, Integrated methods for the construction of threedimensional models and computational probing of structure-function relations in G protein-coupled receptors, in: S.C. Sealfon (Ed.), Methods in Neurosciences, Academic Press, 1995, pp. 366–428.

[45] W.B. Asher, D.S. Terry, G.G.A. Gregorio, A.W. Kahsai, A. Borgia, B. Xie, A. Modak, Y. Zhu, W. Jang, A. Govindaraju, L.Y. Huang, A. Inoue, N.A. Lambert, V. V. Gurevich, L. Shi, R.J. Lefkowitz, S.C. Blanchard, J.A. Javitch, GPCR-mediated beta-arrestin activation deconvoluted with single-molecule precision, Cell. 185 (2022) 1661–1675 e16.

[46] J. Maharana, R. Banerjee, M.K. Yadav, P. Sarma, A.K. Shukla, Emerging structural insights into GPCR-beta-arrestin interaction and functional outcomes, Curr Opin Struct Biol. 75 (2022) 102406.

[47] E. Khoury, L. Nikolajev, M. Simaan, Y. Namkung, S.A. Laporte, Differential regulation of endosomal GPCR/beta-arrestin complexes and trafficking by MAPK, J Biol Chem. 289 (2014) 23302–23317.

[48] D. Dutta, C.D. Williamson, N.B. Cole, J.G. Donaldson, Pitstop 2 is a potent inhibitor of clathrin-independent endocytosis, PLoS One. 7 (2012) e45799.

[49] L. von Kleist, W. Stahlschmidt, H. Bulut, K. Gromova, D. Puchkov, M.J. Robertson, K.A. MacGregor, N. Tomilin, A. Pechstein, N. Chau, M. Chircop, J. Sakoff, J.P. von Kries, W. Saenger, H.-G. Kräusslich, O. Shupliakov, P.J. Robinson, A. McCluskey, V. Haucke, Role of the clathrin terminal domain in regulating coated pit dynamics revealed by small molecule inhibition, Cell. 146 (2011) 471–484.

[50] T. Kirchhausen, E. Macia, H.E. Pelish, Use of dynasore, the small molecule inhibitor of dynamin, in the regulation of endocytosis, Methods Enzymol. 438 (2008) 77–93.

[51] C.-L. Chen, W.-H. Hou, I.-H. Liu, G. Hsiao, S.S. Huang, J.S. Huang, Inhibitors of clathrin-dependent endocytosis enhance TGFbeta signaling and responses, J. Cell Sci. 122 (2009) 1863–1871.

[52] H. Damke, D.D. Binns, H. Ueda, S.L. Schmid, T. Baba, Dynamin GTPase domain mutants block endocytic vesicle formation at morphologically distinct stages, Mol Biol Cell. 12 (2001) 2578–2589.

Published in : Biochemical Pharmacology (2024), vol. 220, 116013
DOI: 10.1016/j.bcp.2023.116013
Status : Postprint (Author's version)

[53] X. Zhao, J. Garcia, L.A. Royer, S. Guo, Colocalization Analysis for Cryosectioned and Immunostained Tissue Samples with or without Label Retention Expansion Microscopy (LR-ExM) by JACoP, Bio Protoc. 12 (2022) e4336.

[54] S. Bolte, F.P. Cordelieres, A guided tour into subcellular colocalization analysis in light microscopy, J Microsc. 224 (2006) 213–232.

[55] B. van Steensel, E.P. van Binnendijk, C.D. Hornsby, H.T. van der Voort, Z. S. Krozowski, E.R. de Kloet, R. van Driel, Partial colocalization of glucocorticoid and mineralocorticoid receptors in discrete compartments in nuclei of rat hippocampus neurons, J Cell Sci. 109 (Pt 4) (1996) 787–792.

[56] M. von Zastrow, B.K. Kobilka, Ligand-regulated internalization and recycling of human beta 2-adrenergic receptors between the plasma membrane and endosomes containing transferrin receptors, J Biol Chem. 267 (1992) 3530–3538.

[57] M. Mauthe, I. Orhon, C. Rocchi, X. Zhou, M. Luhr, K.-J. Hijlkema, R.P. Coppes, N. Engedal, M. Mari, F. Reggiori, Chloroquine inhibits autophagic flux by decreasing autophagosome-lysosome fusion, Autophagy. 14 (2018) 1435–1455.

[58] M.R. Dores, J. Trejo, Ubiquitination of G protein-coupled receptors: functional implications and drug discovery, Mol. Pharmacol. 82 (2012) 563–570.

[59] A.F. Kisselev, A.L. Goldberg, Proteasome inhibitors: from research tools to drug candidates, Chem. Biol. 8 (2001) 739–758.

[60] T. Mund, M.J. Lewis, S. Maslen, H.R. Pelham, Peptide and small molecule inhibitors of HECT-type ubiquitin ligases, Proc. Natl. Acad. Sci. u. s. a. 111 (2014) 16736–16741.

[61] T. Schneider-Poetsch, J. Ju, D.E. Eyler, Y. Dang, S. Bhat, W.C. Merrick, R. Green, B. Shen, J.O. Liu, Inhibition of eukaryotic translation elongation by cycloheximide and lactimidomycin, Nat. Chem. Biol. 6 (2010) 209–217.

[62] S. Lu, W. Jang, A. Inoue, N.A. Lambert, Constitutive G protein coupling profiles of understudied orphan GPCRs, PLoS One. 16 (2021) e0247743.

[63] A. Le Mercier, R. Bonnavion, W. Yu, M.W. Alnouri, S. Ramas, Y. Zhang, Y. Jäger, K. A. Roquid, H.-W. Jeong, K.K. Sivaraj, H. Cho, X. Chen, B. Strilic, T. Sijmonsma, R. Adams, T. Schroeder, M.A. Rieger, S. Offermanns, GPR182 is an endotheliumspecific atypical chemokine receptor that maintains hematopoietic stem cell homeostasis, Proc. Natl. Acad. Sci. U. S. A. 118 (2021) e2021596118.

[64] J. Wess, Molecular basis of receptor/G-protein-coupling selectivity, Pharmacol. Ther. 80 (1998) 231–264.

[65] Z. Yang, F. Yang, D. Zhang, Z. Liu, A. Lin, C. Liu, P. Xiao, X. Yu, J.-P. Sun, Phosphorylation of G Protein-Coupled Receptors: From the Barcode Hypothesis to the Flute Model, Mol. Pharmacol. 92 (2017) 201–210.

[66] X.E. Zhou, Y. He, P.W. de Waal, X. Gao, Y. Kang, N. Van Eps, Y. Yin, K. Pal, D. Goswami, T.A. White, A. Barty, N.R. Latorraca, H.N. Chapman, W.L. Hubbell, R. O. Dror, R.C. Stevens, V. Cherezov, V.V.

Published in : Biochemical Pharmacology (2024), vol. 220, 116013
DOI: 10.1016/j.bcp.2023.116013
Status : Postprint (Author's version)

Gurevich, P.R. Griffin, O.P. Ernst, K. Melcher, H.E. Xu, Identification of Phosphorylation Codes for Arrestin Recruitment by G Protein-Coupled Receptors, Cell. 170 (2017) 457–469.e13.

[67] Y. Kang, X.E. Zhou, X. Gao, Y. He, W. Liu, A. Ishchenko, A. Barty, T.A. White, O. Yefanov, G.W. Han, Q. Xu, P.W. de Waal, J. Ke, M.H.E. Tan, C. Zhang, A. Moeller, G.M. West, B.D. Pascal, N. Van Eps, L.N. Caro, S.A. Vishnivetskiy, R. J. Lee, K.M. Suino-Powell, X. Gu, K. Pal, J. Ma, X. Zhi, S. Boutet, G.J. Williams, M. Messerschmidt, C. Gati, N.A. Zatsepin, D. Wang, D. James, S. Basu, S. Roy-Chowdhury, C.E. Conrad, J. Coe, H. Liu, S. Lisova, C. Kupitz, I. Grotjohann, R. Fromme, Y. Jiang, M. Tan, H. Yang, J. Li, M. Wang, Z. Zheng, D. Li, N. Howe, Y. Zhao, J. Standfuss, K. Diederichs, Y. Dong, C.S. Potter, B. Carragher, M. Caffrey, H. Jiang, H.N. Chapman, J.C.H. Spence, P. Fromme, U. Weierstall, O.P. Ernst, V. Katritch, V.V. Gurevich, P.R. Griffin, W.L. Hubbell, R.C. Stevens, V. Cherezov, K. Melcher, H.E. Xu, Crystal structure of rhodopsin bound to arrestin by femtosecond X-ray laser, Nature. 523 (2015) 561–567.

[68] J. Maharana, P. Sarma, M.K. Yadav, S. Saha, V. Singh, S. Saha, M. Chami, R. Banerjee, A.K. Shukla, Structural snapshots uncover a key phosphorylation motif in GPCRs driving beta-arrestin activation, Mol Cell. (2023), https://doi.org/10.1016/j.molcel.2023.04.025.

[69] P. Isaikina, I. Petrovic, R.P. Jakob, P. Sarma, A. Ranjan, M. Baruah, V. Panwalkar, T. Maier, A.K. Shukla, S. Grzesiek, A key GPCR phosphorylation motif discovered in arrestin2·CCR5 phosphopeptide complexes, Mol. Cell. (2023), https://doi.org/10.1016/j.molcel.2023.05.002.

[70] O. Sveidahl Johansen, T. Ma, J.B. Hansen, L.K. Markussen, R. Schreiber, L. Reverte- Salisa, H. Dong, D.P. Christensen, W. Sun, T. Gnad, I. Karavaeva, T.S. Nielsen, S. Kooijman, C. Cero, O. Dmytriyeva, Y. Shen, M. Razzoli, S.L. O'Brien, E. N. Kuipers, C.H. Nielsen, W. Orchard, N. Willemsen, N.Z. Jespersen, M. Lundh, E. G. Sustarsic, C.M. Hallgren, M. Frost, S. McGonigle, M.S. Isidor, C. Broholm, O. Pedersen, J.B. Hansen, N. Grarup, T. Hansen, A. Kjær, J.G. Granneman, M. M. Babu, D. Calebiro, S. Nielsen, M. Rydén, R. Soccio, P.C.N. Rensen, J.T. Treebak, T.W. Schwartz, B. Emanuelli, A. Bartolomucci, A. Pfeifer, R. Zechner, C. Scheele, S. Mandrup, Z. Gerhart-Hines, Lipolysis drives expression of the constitutively active receptor GPR3 to induce adipose thermogenesis, Cell. 184 (2021) 3502–3518.e33.

[71] S. Rajagopal, S.K. Shenoy, GPCR desensitization: Acute and prolonged phases, Cell. Signal. 41 (2018) 9–16.

[72] D. Calebiro, V.O. Nikolaev, L. Persani, M.J. Lohse, Signaling by internalized Gprotein- coupled receptors, Trends Pharmacol. Sci. 31 (2010) 221–228.

[73] M.J. Lohse, K.P. Hofmann, Spatial and Temporal Aspects of Signaling by G-Protein- Coupled Receptors, Mol. Pharmacol. 88 (2015) 572–578.

[74] A. Marchese, J. Trejo, Ubiquitin-dependent regulation of G protein-coupled receptor trafficking and signaling, Cell. Signal. 25 (2013) 707–716.

[75] D. Calebiro, Z. Koszegi, The subcellular dynamics of GPCR signaling, Mol. Cell. Endocrinol. 483 (2019) 24–30.

Published in : Biochemical Pharmacology (2024), vol. 220, 116013
DOI: 10.1016/j.bcp.2023.116013
Status : Postprint (Author's version)

[76] B. Holst, A. Cygankiewicz, T.H. Jensen, M. Ankersen, T.W. Schwartz, High constitutive signaling of the ghrelin receptor–identification of a potent inverse agonist, Mol. Endocrinol. 17 (2003) 2201–2210.